Journal of Organometallic Chemistry, 401 (1991) 91–123
Elsevier Sequoia S.A., Lausanne
JOM 21208

The solution structure and fluxional behaviour of cyclic and acyclic (diene)Fe(CO)$_2$L complexes (L = phosphine, phosphite, isonitrile)

James A.S. Howell *, Gary Walton, Marie-Claire Tirvengadum, Adrian D. Squibb, Michael G. Palin
Chemistry Department, University of Keele, Keele, Staffordshire ST5 5BG (U.K.)

Patrick McArdle, Desmond Cunningham,
Chemistry Department, University College, Galway (Ireland)

Zeev Goldschmidt, Hugo Gottlieb and Gila Strul,
Chemistry Department, Bar Ilan University, Ramat Gan (Israel)

(Received June 18th, 1990)

Abstract

Variable temperature ^{13}C and ^{31}P NMR spectroscopy has been used to establish solution structures and conformer populations for a variety of cyclic and acyclic (diene)Fe(CO)$_2$L complexes (L = phosphine, phosphite, isonitrile). The solid state structures of (2,3-dimethylbutadiene)Fe(CO)$_2$PPh$_3$ and (*trans,trans*-2,4-hexadiene)Fe(CO)$_2$PPh$_3$ have been determined and used as a basis for molecular modelling of steric effects in these complexes.

Diene and dienyl complexes of tricarbonyliron continue to attract attention as synthetic intermediates, particularly for enantioselective synthesis. Though the chemistry of cyclic six- and seven-membered ring complexes has already been developed extensively [1a–c], there has been a recent renewed interest in the use of acyclic diene complexes targetted towards several molecules of pharmacological interest [2]. The ease of preparation of related (diene)Fe(CO)$_2$L derivatives (L = phosphine, phosphite) [3a–c] provides alternative complexes which exhibit increased reactivity towards electrophiles and cycloaddition, [4a–c] altered and increased regiospecificity in nucleophilic attack [4b,5a,b], and the potential for resolution or asymmetric induction via the use of chiral auxiliary ligands [4b,6a–d].

Particularly in the case of regiospecificity, such changes may be the result of site preference of the auxiliary ligand for non-equivalent sites within the square pyramidal molecular structure. We wish to report here NMR and single crystal studies which establish the solid-state and solution structures of a variety of simple diene-substituted cyclic and acyclic (diene)Fe(CO)$_2$L complexes (L = phosphine, phosphite, isonitrile), together with molecular modelling studies which at least for the most sterically demanding PPh_3 complexes, provide some discrimination between steric and electronic effects [7].

Though a number of experimental studies have been reported on fluxional processes in (diene)$M(CO)_3$ complexes (M = Fe, Ru, Os) [8a–g], systematic studies of (diene)$M(CO)_2L$ complexes are less numerous and confined to cases where $L = PF_3$ [9a,b], isonitrile [10a–d] and $P(OCH_2)_3CEt$ [8f] and to phosphine and phosphite substituted (η^4-enone)$Fe(CO)_2L$ derivatives [11a,b].

Results

(i) Preparation and fluxionality

The phosphine, arsine, stibine and isonitrile complexes **1–7**, **9–17** and **20–27**

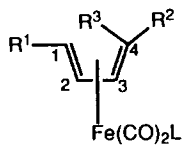

	R^1	R^2	R^3	L
(1)	H	H	H	PPh_3
(2)	H	Me	H	PPh_3
(3)	H	H	Me	PPh_3
(4)	Me	Me	H	PPh_3
(5)	H	Ph	H	PPh_3
(6)	Me	CO_2Me	H	PPh_3
(7)	Me	CHO	H	PPh_3
(8)	Me	CHO	H	$P(OMe)_3$

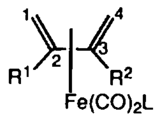

	R^1	R^2	L
(9)	Me	Me	PPh_3
(10)	H	Me	PPh_3
(11)	H	Me	PPh_2Me
(12)	H	Me	$PPhMe_2$
(13)	H	Me	$AsPh_3$
(14)	H	Me	$SbPh_3$
(15)	H	Me	CNMe
(16)	H	Me	CNEt
(17)	H	Me	$CNBu^t$
(18)	H	Me	$P(OMe)_3$

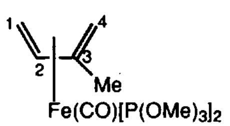

(19)

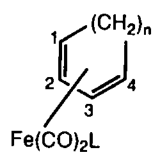

	n	L
(20)	2	PPh_3
(21)	3	PPh_3
(22)	2	CNMe
(23)	3	CNMe
(24)	2	CNEt
(25)	3	CNEt
(26)	2	$CNBu^t$
(27)	3	$CNBu^t$
(28)	3	$P(OMe)_3$
(29)	3	$P(OPh)_3$

were prepared by substitution of the tricarbonyl in the presence of Me_3NO [3a]. The phosphite complexes **8**, **18** and **19** were prepared photolytically, while **28** and **29** were prepared by direct thermal substitution of the tricarbonyl [5a].

Satisfactory analytical and spectroscopic data were obtained for all complexes. (Tables 1 and 2) Though a small number of the complexes have been previously prepared, variable temperature NMR studies have been reported only on **24**, a complex where our conclusions differ from those previously published [10b].

Proton spectra of these complexes (relative to the tricarbonyl) show consistent shielding of the terminal diene hydrogens. There is no clearly consistent trend in the shielding of the averaged room temperature chemical shifts of the diene carbons, nor in the magnitude of the long range P–C and P–H coupling constants. P–C coupling is confined exclusively to the terminal diene carbons; P–H coupling is observed to both terminal and internal hydrogen, but for acyclic complexes is strongest to H_a protons. Small long range P–C coupling to the methyl substituent is also observed in the isoprene complexes **10–12** and **18**. All complexes show a deshielding of both axial and basal CO resonances [12*] which increases in the order CNR $\hat{=}$ $P(OR)_3 < PR_3$; for phosphine complexes, P–CO coupling constants provide a reliable aid to structure elucidation in the low temperature limiting spectra and have the values J(Paxial–CObasal) $\hat{=}$ 5 Hz, J(Pbasal–COaxial) $\hat{=}$ 4 Hz and J(Pbasal–CObasal) $\hat{=}$ 25 Hz. Couplings for phosphite complexes are in the same order, but slightly larger.

The fluxional process in these $Fe(CO)_2L$ complexes can be represented in the following way:

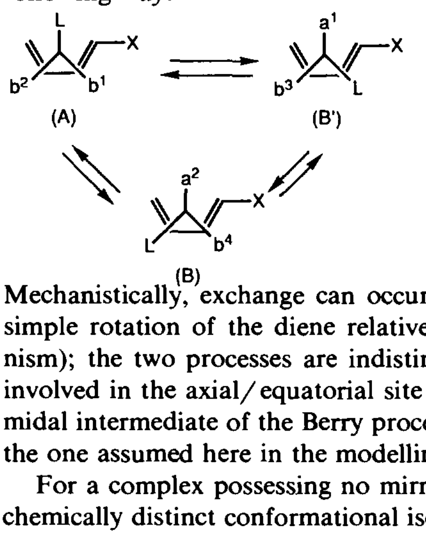

Mechanistically, exchange can occur by either sequential Berry pseudorotation or simple rotation of the diene relative to the $Fe(CO)_2L$ fragment (turnstile mechanism); the two processes are indistinguishable by NMR [13a,b]. Because of strain involved in the axial/equatorial site occupancy of the diene in the trigonal bipyramidal intermediate of the Berry process, the turnstile mechanism is preferred, and is the one assumed here in the modelling studies.

For a complex possessing no mirror plane (e.g. X = Me), **A**, **B** and **B′** represent chemically distinct conformational isomers in which two non-interconverting sets of CO ligands ($b^1/b^3/a^2$ and $b^2/a^1/b^4$) undergo exchange. The appearance of the averaged ^{13}C spectrum will depend on the identities and relative populations of the conformers, but exchange does not completely average the CO resonances and two averaged resonances are observed for all compounds of this type, with the exception of the isonitrile complex **15**. For complexes possessing a mirror plane (e.g. X = H), **B** and **B′** form an enantiomeric pair, and complete carbonyl scrambling occurs,

* Reference number with asterisk indicates a note in the list of references.

Table 1

^{13}C and ^{31}P NMR spectral data [a]

Complex	Averaged spectrum (20 °C)		Limiting low temperature spectrum			Temperature (°C)	Isomer ratio
			A	B	B′		
1	1,4	40.6 [40.7] [b]	[d]	33.9, 43.4		−85	**A**:**B**/**B′** = 1:6
	2,3	84.3 [85.5]		80.9, 84.6			
	CO	217.8 (13.9)		215.1 (26.2)			
	PPh_3	[c]		221.1 (3.6)			
	P	71.9	76.5	72.3			
2	1	42.7 (6.9) [39.4]	[e]	[e]		−90	**A**:**B** = 1:18
	2	82.2 [80.9]					
	3	86.6 [89.0]					
	4	52.8 (7.9) [58.5]					
	Me	19.0					
	CO	215.8 (23.4)					
		221.2 (4.9)					
	P	71.6	73.2	72.2			
3	1	40.8 [40.9]		43.5	35.8	−85	**B**:**B′** = 2.5:1
	2	90.1 [90.4]		91.6	89.6		
	3	86.9 [88.2]		85.4	87.3		
	4	49.7 (4.9) [53.9]		47.3 (8.8)	48.1 (br)		
	Me	13.8		14.4	13.6		
	CO	217.8 (16.6)		215.8 (25.5)	215.3 (26.5)		
		219.0 (10.7)		222.4 (br)	222.9 (4.9)		
	P	68.9		68.4	71.1		
4	1,4	58.1 (3.6) [56.9]	[e]	[e]		−85	**A**:**B**/**B′** = 52:1
	2,3	85.3 [84.8]					
	Me	17.7					
	CO	217.1 (4.9)					
	P	68.0	69.1	66.3			
5	1	43.3 (6.8) [38.8]	[e]	[e]		−85	**A**:**B** = 1:13
	2,3	81.6, 82.6 [81.2, 82.1]					
	4	56.2 (5.9) [59.4]					
	Ph	142.1 (α)					
		128.0 (β)					
		125.9 (γ)					
		124.9 (δ)					
	CO	214.8 (23.4)					
		220.4 (5.9)					
	P	71.6	68.2	72.5			
6	1	61.8 [59.6]	[e,f]			−85	axial only
	2	88.6 [88.3]					
	3	83.6 [82.8]					
	4	48.5 (5.9) [45.6]					
	Me	18.3					
	CO_2Me	50.6, 174.1					
	CO	211.8 (5.9)					
		214.6 (8.8)					
	P	64.9					

Table 1 (continued)

Complex	Averaged spectrum (20 °C)		Limiting low temperature spectrum A	B	B′	Temperature (°C)	Isomer ratio
7	1,4	61.7 (1.9) [60.3]	[e]	[e]		−60	**A**:**B**/**B′** = 32:1
		59.3 (4.9) [54.5]					
	2	90.4 [89.5]					
	3	82.3 [81.2]					
	Me	18.1					
	CHO	197.5					
	CO	211.7 (4.9)					
		214.8 (8.8)					
	P	63.8	64.0	58.8			
8	1,4	54.9	[e]	[e]	[c]	−60	**A**:**B**:**B′** = 1:4:22
		57.6					
	2	88.5					
	3	80.3					
	Me	17.8					
	CHO	197.2					
	CO	210.5 (br)					
		212.8 (16.8)					
	P	182.6	183.3	181.9	182.9		
9	1,4	47.5	[e,f]			−85	axial only
	2,3	98.3					
	Me	19.8					
	CO	214.1 (4.9)					
	P	74.8					
10	1	41.6 (5.3) [37.4]	35.9	43.1		−100	**A**:**B** = 1
	2	86.1 [84.1]	84.2	86.1			
	3	100.4 [102.4]	97.9	101.6			
	4	42.7 [43.1]	40.0	48.0			
	Me	22.0	21.1	22.3			
	CO	214.9 (16.1)	213.7 (3.2)	214.6 (25.6)			
		218.2 (4.3)	213.9 (5.3)	221.7 (6.4)			
	P	74.4	73.3	77.1			
11	1	40.4 (5.9)	37.3	40.8 (br)		−85	**A**:**B** = 2:1
	2	84.9	84.9	[g]			
	3	100.5	102.2	98.2			
	4	43.5	41.8	47.6 (br)			
	Me	22.8	23.7	22.9			
	CO	214.7 (13.7)	214.3 (4.9)	215.0 (31.8)			
		217.0 (5.9)	214.4 (br)	222.5 (4.9)			
	PPh_2Me	19.7 (28.3)					
		128.2 (9.3) (γ)					
		129.5 (3.0) (δ)					
		131.5 (10.9) (β)					
		138.7 (38.0) (α)					
		138.8 (38.0) (α′)					
	P	53.3	53.3	56.7			
12	1	38.9 (5.9)	39.9 (5.9)	37.2 (5.6)		−85	**A**:**B** = 5:1
	2	84.3	84.0	85.4			
	3	100.6	101.7	98.7			
	4	43.1 (3.0)	45.8 (7.8)	38.7 (br)			
	Me	23.0	22.8	23.1			
	CO	214.3 (12.6)	213.9 (6.8)	215.1 (29.3)			
		215.8 (6.9)	214.4 (7.8)	222.2 (5.8)			

(continued)

Table 1 (continued)

Complex	Averaged spectrum (20 °C)		Limiting low temperature spectrum			Temperature (°C)	Isomer ratio
			A	B	B′		
12	$PPhMe_2$	19.5 (24.0)					
		19.6 (24.0)					
		129.0 (9.0) (γ)					
		128.2 (2.0) (δ)					
		127.8 (8.8) (β)					
		141.0 (29.1) (α)					
	P	35.6	36.6	37.7			
13	1	39.2	40.6	36.7		−85	**A**:**B** = 6:1
	2	84.8	84.8	85.0			
	3	100.5	101.8	98.0			
	4	43.1	45.9	39.5			
	Me	22.9	23.6	22.8			
	CO	214.3	213.9	215.6			
		215.9	214.0	222.1			
	$AsPh_3$	137.4 (α)					
		132.6 (β)					
		129.2 (δ)					
		128.4 (γ)					
14	1	35.1	[e]			−80	axial only
	2	82.5					
	3	99.4					
	4	40.8					
	Me	22.6					
	CO	213.8					
		214.4					
	$SbPh_3$	127.9 (δ)					
		128.7 (γ)					
		135.1 (β)					
		135.9 (α)					
15	1	35.1	36.1	36.8	37.2	−75	**A**:**B**:**B′** = 1:5:5
	2	83.5	82.2	81.6	83.7		
	3	100.8	99.9	99.6	100.5		
	4	41.3	[d]	42.4 (br)	[g]		
	Me	22.0	[d]	22.1	22.4		
	CO	216.2	212.1	219.5	[g]		
			212.4	213.4	213.9		
	MeNC	29.7 (br)	[d]	29.6	31.6		
		163.4 (br)	162.4	157.1	158.5		
16	1	35.0	[h]	[h]	[h]	−75	**A**:**B**:**B′** = 1:5:8
	2	83.4	82.2	81.5	83.7		
	3	100.8	99.8	100.3	99.5		
	4	41.4	[h]	[h]	[h]		
	Me	22.9	[d]	22.1	22.4		
	CO	216.1	212.2	219.5	[g]		
		216.5	212.4	213.8	213.4		
	EtNC	15.6	[d]	14.9	14.6		
		39.4 (br)	[h]	[h]	[h]		
		163.4 (br)	161.8	158.2	156.8		

Complex	Averaged spectrum (20 °C)		Limiting low temperature spectrum A	B	B′	Temperature (°C)	Isomer ratio
17	1	39.2		36.7 (br)	[g]	−80	**B** : **B′** = 1 : 3
	2	82.6		80.9	83.2		
	3	100.1		99.6	99.3		
	4	41.2		42.1	[g]		
	Me	22.4		21.6	[g]		
	CO	215.5		219.1	[g]		
		216.6		213.4	212.9		
	Bu^tNC	30.1		29.1	31.2		
		161.1 (br)		156.5	155.5		
18	1	35.8 (6.7)	36.2	37.2 (10.7)	[d]	−105	**A** : **B** : **B′** = 8 : 17 : 1
	2	82.2	82.4	[g]			
	3	99.2	100.3	98.7			
	4	40.5	42.1	38.5 (14.8)			
	Me	21.4	22.1	[g]			
	CO	213.9 (20.2)	212.1 (br)	212.1 (34.9)			
		216.4 (10.8)		220.1 (12.1)			
	$P(OMe)_3$	51.1 (2.9)					
	P	189.9	197.5	189.4	187.5		
20	1,4	61.5 (3.0) [61.1]		[e,f]			basal only
	2,3	84.6 [84.3]					
	CH_2	24.7					
	CO	218.7 (13.6)					
	P	70.2					
21	1,4	57.3 [59.5]		60.4,[j]		−85	basal only
	2,3	87.8 [87.9]		85.5, 89.7			
	$CH_2(\alpha)$	28.5		28.5 (br)			
	$CH_2(\beta)$	24.5		24.4			
	CO	218.9 (13.8)		216.2 (24.4)			
				222.7 (br)			
	P	70.3		[f]			
22	1,4	58.6	58.6	60.2		−85	**A** : **B**/**B′** = 1 : 7
	2,3	84.7	82.4	82.9, 85.2			
	CH_2	24.1	23.1 (br)	[g]			
	CO	216.5	213.3	214.7			
				218.9			
	MeNC	29.7 (br)	30.5	29.6			
		[k]	163.4	157.5			
23	1,4	55.7	[d]	58.7,[j]		−80	**A** : **B**/**B′** = 1 : 10
	2,3	87.2	[d]	86.4, 88.5			
	$CH_2(\alpha)$	28.1	[d]	27.9, 28.2			
	$CH_2(\beta)$	24.4	[d]	24.3			
	CO	216.4	213.2	214.7			
				220.8			
	MeNC	29.8 (br)	30.7	30.6			
		164.2 (br)	167.9	159.1			
24	1,4	58.6	58.4	60.3		−80	**A** : **B**/**B′** = 1 : 3
	2,3	84.7	82.3	83.0, 85.4			
	CH_2	24.1	22.5	23.2			
	CO	216.6	213.4	214.7			
				219.1			
	EtNC	15.6	14.5	14.5			
		39.3 (br)	38.6	38.6			
		[k]	162.9	157.3			

(continued)

Table 1 (continued)

Complex	Averaged spectrum (20 °C)		Limiting low temperature spectrum A	B	B′	Temperature (°C)	Isomer ratio
25	1,4	55.8	[d]	57.5, [j]		−80	**A**:**B**/**B′** = 1:8
	2,3	87.3	[d]	85.5, 87.7			
	$CH_2(\alpha)$	28.2	26.6	27.0, 27.2			
	$CH_2(\beta)$	24.4	[d]	23.3			
	CO	216.4	212.2	212.2			
				213.7			
	EtNC	15.6	15.3	14.7			
		39.3 (br)	38.7	38.6			
		164.3 (br)	166.5	157.8			
26	1,4	58.7	58.3	60.4		−85	**A**:**B**/**B′** = 1:2
	2,3	84.7	82.2	83.2, 85.6			
	CH_2	24.2	23.1	[g]			
	CO	216.5	213.5	214.8			
				219.1			
	Bu^tNC	30.7	29.4	[g]			
		[k]	161.3	156.5			
27	1,4	55.7	55.3	55.6, 57.6		−85	**A**:**B**/**B′** = 1:5
	2,3	87.2	85.1	85.5, 87.7			
	$CH_2(\alpha)$	28.2	26.4	26.8, 27.1			
	$CH_2(\beta)$	24.5	23.2	23.2			
	CO	216.3	212.4	213.4			
				220.0			
	Bu^tNC	30.7	30.1	29.4			
		[k]	164.7	156.9			
28	1,4	57.0		57.9, [j]		−85	basal only
	2,3	86.4		85.5, 87.8			
	$CH_2(\alpha)$	28.1		27.8			
	$CH_2(\beta)$	24.3		24.2			
	CO	217.3 (20.4)		213.6 (34.2)			
				221.8 (7.8)			
	$P(OMe)_3$	50.9		50.7			
	P	184.0		[f]			
29	1,4	58.4 (4.9)		60.0 (7.8), [j]		−80	basal only
	2,3	86.3		85.2, 87.2			
	$CH_2(\alpha)$	27.9		27.8			
	$CH_2(\beta)$	24.1		23.9			
	CO	216.0 (18.5)		212.8 (31.3)			
				219.9 (3.9)			
	$P(OPh)_3$	151.5 (5.9) (α)					
		129.6 (β)					
		124.6 (δ)					
		121.3 (5.0) (γ)					
	P	169.0		[f]			
19			1	35.5			
				(t, 9.8, 9.8) [l]	[d,m]		
			2	80.1			
			3	95.9			
			4	38.6			
				(dd, 9.3, 16.1)			

Table 1 (continued)

Complex	Averaged spectrum (20 °C)	Limiting low temperature spectrum A	B	B′	Temperature (°C)	Isomer ratio
19		Me	22.2			
		CO	213.6			
			(dd, 8.8, 40)			
		$P(OMe)_3$	49.5			
			49.9 (3.0)			
		P	204.0			**AB**:**AB′**
			(J(P–P)			= 38:1(J(P–P)
			= 23.4)203.3	=16.1)		
			188.5	185.6		

[a] ^{13}C chemical shifts in ppm relative to TMS; ^{31}P chemical shifts in ppm relative to 85% H_3PO_4; spectra in CD_2Cl_2/CH_2Cl_2 solvent; J(P–C) values in parentheses. [b] Values for (diene)$Fe(CO)_3$ complex given in square brackets. [c] 136.7(37.6) (α), 133.1(10.8) (β), 129.4(2.7) (δ), 128.0(9.4) (γ), other PPh_3 complexes are similar. [d] ^{13}C resonances for minor isomer not seen. [e] ^{13}C spectrum essentially invariant with temperature. [f] ^{31}P spectrum essentially invariant with temperature. [g] Coincident resonance. [h] Overlap of C(1,4) and CH_2 resonances. [j] Under solvent resonance at 53.8. [k] CN resonance not seen at +20 °C. [l] Major AB isomer. [m] Minor AB′ isomer.

though the position and coupling constant of the averaged resonance will also depend on the relative populations of axial and basal conformers.

(ii) Solution structures of the phosphine complexes

Solution structures were established using variable temperature ^{31}P and ^{13}C spectroscopy; the results are summarized in Table 1. The sorbaldehyde complexes **7** and **8** exhibit additional low temperature restricted rotation about the C–CHO bond, and are discussed separately, together with the methylsorbate complex **6**.

The asymmetric complexes **2**, **3**, **5** and **10–12** all exhibit two ^{31}P resonances of varying relative intensity in the limiting low temperature spectra which are averaged to a single resonance at 20 °C. Spectra of (isoprene)$Fe(CO)_2PPh_3$ (**10**) are shown in Fig. 1. The two ^{31}P resonances of equal intensity may be assigned to axial and basal conformers on the basis of the ^{13}C spectrum which shows clearly axial/basal and basal/basal pairs of resonances. The single basal conformer is assigned to **B** rather than **B′** on the basis of modelling studies (vide infra) and on the basis of the low temperature ^1H spectrum (−98 °C, CD_2Cl_2):

	4s	*4a*	*2*	*1s*	*1a*	*Me*
A	1.75	−1.26	5.28	1.55	−1.66	2.23
	J(*4a*–P) = 11,		J(*1s*–P) = 3,		J(*1a*–P) = 8.5	
B	1.62	0.14	4.09	0.63	−0.05	2.11
	J(*1s*–P) = 6					

Of particular note are the large upfield shifts for *1a*, *4a* in **A** and *1s*, *2* in **B** attributable to shielding by PPh_3 and the strong P–H coupling to *1a*, *4a*, *1s* of **A** and *1s* of **B** as a result of small P–Fe–C–H dihedral angles. Conformer interconversion results in b^2/a^2 and b^1/b^4 CO exchange to yield two averaged ^{13}C resonances whose chemical shifts and coupling constants are in agreement with prediction.

The ^{13}C spectrum of (*trans*-pentadiene)Fe(CO)$_2$PPh$_3$ (**2**) is essentially temperature invariant and consistent with only basal conformer being present (assigned to **B**

Table 2

^{1}H NMR [a] infrared [b] and analytical data

Complex	^{1}H NMR		Infrared (cm^{-1})	Analysis		
				CHN (found)	CHN (calc)	M.p. (°C)
1	1,4*a*	−0.11 (m) [−0.03] [c]	1983	67.1	67.3	146–147
		$J(a-s)$ = 2.1, $J(a-P)$ = 4.3	1927	5.13	4.91	
	1,4*s*	1.35 (m) [1.46]				
		$J(s-P)$ = 2.1				
	2,3	4.83 (m) [4.89]				
		$J(a-2,3)$ = 7.9, $J(s-2,3)$ = 5.3				
		$J(P-2,3)$ = 1.8				
	PPh_3	[d]				
2	1*a*	−0.01 (t)	1976	67.8	67.9	99–101
	1*s*	0.97 (m)	1918	5.09	5.13	
	4*a*	0.72 (m)				
	2	4.35 (m)				
	3	4.98 (m)				
	Me	1.42 (dd, 6.3, 1.4)				
3	1*a*	1.15 (m)	1914	68.5	67.9	106–107
	1*s*	1.62 (m)	1904	5.36	5.13	
	4*s*	2.42 (m)				
	2	4.92 (m)				
	3	4.70 (m)				
	Me	0.82 (d)				
		$J(4s-Me)$ = 7.2				
4	1,4*a*	−0.12 (m)	1974	68.7	68.4	136–138
		$J(a-2,3)$ = 7.4, $J(a-P)$ = 8.6	1914	5.82	5.48	
	2,3	4.94 (m)				
	Me	1.25 (d)				
		$J(a-Me)$ = 6.2				
5	1*a*	0.21 (m)	1982	71.3	71.4	132–133
	1*s*	1.21 (m)	1928	4.90	4.96	
	4*a*	1.66 (d)				
	2	4.53 (m)				
	3	5.62 (m)				
	Ph	[e]				
6	1*a*	−0.28 (m)	1986	64.9	64.8	158–160
	4*a*	0.09 (m)	1924	5.07	5.00	
	2	4.59 (m)				
	3	5.87 (m)				
	Me	1.03 (d, 6.1)				
	CO_2Me	3.19 (s)				
7	1,4*a*	0.16 (m) [0.75]	1986	66.2	66.4	143–144
	2	4.62 (m) [4.29]	1930	4.96	4.89	
	3	5.31 (m) [5.10]				
	Me	1.04 (d, 6.2)				
	CHO	9.10 (d, 5.6)				

Table 2 (continued)

Complex	^{1}H NMR		Infrared (cm^{-1})	Analysis		
				CHN (found)	CHN (calc)	M.p. (°C)
8	1*a*	1.04 (m)	1999	39.7	39.8	55–57
	4*a*	0.89 (m)	1935	5.48	5.12	
	2	4.57 (m)				
	3	5.16 (m)				
	Me	1.26 (dd, 6.1, 1.3)				
	CHO	9.20 (d, 6.1)				
	$P(OMe)_3$	3.28 (d, 11.4)				
9	1,4*a*	-0.92 (dd)	1980	68.7	68.4	116–118
		J(P–1,4) = 11.0,				
		J(*a*–*s*) = 1.1	1920	5.57	5.48	
	1,4*s*	1.59 (d)				
	Me	2.06 (d, 2.2)				
10	1*a*	−0.35 (td) [0.0]	1980	67.6	67.9	122–124
		J(1*a*–1*s*) = 2.1,	1922	5.20	5.13	
		J(1*a*–P) = 9.1				
	4*a*	−0.10 (m) [0.30]				
		J(4*a*–4*s*) = 2.1,				
		J(4*a*–P) = 3.9				
	1*s*	1.40 (m) [1.63]				
		J(1*s*–P) = 4.6				
	4*s*	1.81 (t) [1.80]				
		J(4*s*–P) = 1.7				
	2	4.81 (t) [5.26]				
		J(1*a*–2) = 9.1,				
		J(1*s*–2) = 7.0				
	Me	2.17 (d, 0.6)				
11	1*a*	−0.59 (m)	1978	63.7	63.2	100 °C/0.04 mmHg
	4*a*	−0.28 (m)	1922	5.76	5.53	
	1*s*	1.28 (m)				
	4*s*	1.70 (m)				
	2	4.95 (t)				
	Me	2.16 (d, 1.2)				
	PPh_2Me	1.80 (d, 7.4)				
		7.2–7.7 (m)				
12	1*a*	−0.81 (m)	1974	57.3	56.6	85 °C/0.04 mmHg
	4*a*	−0.50 (m)	1918	6.02	5.97	
	1*s*	1.16 (m)				
	4*s*	1.47 (m)				
	2	4.81 (t)				
	Me	2.02 (d, 1.5)				
	$PPhMe_2$	1.36 (d, 8.1)				
		7.1–7.6 (m)				
13	1*a*	−0.65 (dd)	1970	61.4	61.7	84–86
	4*a*	−0.39 (m)	1908	4.97	4.73	
	1*s*	1.46 (dd)				
	4*s*	1.69 (m)				
	2	4.96 (t)				
	Me	2.04 (s)				
	$AsPh_3$	7.01–7.61 (m)				

(continued)

Table 2 (continued)

Complex	^{1}H NMR		Infrared (cm^{-1})	Analysis		
				CHN (found)	CHN (calc)	M.p. (°C)
14	1*a*	−0.71 (dd)	1976	56.7	56.3	85–87
	4*a*	−0.45 (m)	1912	4.20	4.32	
	1*s*	1.51 (dd)				
	4*s*	1.67 (m)				
	2	5.12 (t)				
	Me	2.12 (s)				
	$SbPh_3$	7.07–7.71 (m)				
15	1*a*	−0.20 (dd)	2138 [f]	49.0	48.9	40°C/0.1 mmHg
		$J(1a-2) = 8.4$,	1990	5.18	4.98	
		$J(1a-1s) = 2.2$	1946	5.92	6.34	
	4*a*	0.07 (dd)				
		$J(4a-4s) = 2.0$,				
		$J(4a-2) = 0.9$				
	1*s*	1.42 (dd)				
		$J(1s-2) = 6.7$				
	4*s*	1.56 (t)				
		$J(4s-2) = 1.8$				
	2	4.98 (t)				
	Me	1.96 (s)				
	MeNC	1.90 (s)				
16	1*a*	−0.17 (dd)	2128 [f]	51.1	51.1	40°C/0.1 mmHg
	4*a*	0.11 (m)	1992	5.73	5.54	
	1*s*	1.43 (dd)	1944	6.06	5.96	
	4*s*	1.57 (t)				
	2	5.03 (t)				
	Me	1.96 (s)				
	EtNC	0.43 (t)				
		2.35 (q, $J = 7.4$)				
17	1*a*	−0.19 (dd)	2103 [f]	54.8	54.7	40°C/0.1 mmHg
	4*a*	0.11 (t)	1992	6.66	6.47	
	1*s*	1.42 (dd)	1944	5.16	5.33	
	4*s*	1.56 (t)				
	2	4.99 (t)				
	Me	1.98 (s)				
	Bu^tNC	0.77 (s)				
18	1*a*	−0.14 (td)	1990	39.2	39.5	55°C/0.1 mmHg
		$J(1a-1s) = 2.3$,	1932	5.40	5.59	
		$J(1a-P) = 9.3$				
	4*a*	0.19 (m)				
		$J(4a-4s) = 1.7$,				
		$J(4a-P) = 5.8$				
	1*s*	1.59 (m)				
		$J(1s-P) = 4.1$				
	4*s*	1.74 (m)				
		$J(4s-P) = 1.6$				
	2	5.00 (t)				
		$J(1a-2) = 9.2$,				
		$J(1s-2) = 6.7$				
	Me	2.06 (d, 1.9)				
	$P(OMe)_3$	3.36 (d, 11.5)				

Table 2 (continued)

Complex	^{1}H NMR		Infrared (cm^{-1})	Analysis CHN (found)	CHN (calc)	M.p. (°C)
19	1*a*	−0.48 (m)	1910	36.2	36.0	40 °C/0.01 mmHg
	4*a*	−0.06 (m)		6.60	6.50	
	1*s*, 4*s*	1.73 (m)				
	2	5.00 (m)				
	Me	2.22 (d, 2.8)				
	$P(OMe)_3$	3.45 (dd, 11.2, 7.7)				
20 [g]	1,4	2.62 (m) [2.69]	1975	69.1	68.7	118–120
	2,3	4.80 (dd) [4.57]	1922	4.81	5.07	
		$J(P-2,3) = 3.9$,				
		$J_{1-2} = 3.0$				
	CH_2(*exo*)	1.40 (d)				
	CH_2(*endo*)	1.86 (d)				
		$J(exo-endo) = 10.2$				
21	1,4	2.57 (m)	1972	68.7	69.2	132–134
	2,3	4.62 (m)	1918	5.25	5.34	
	$CH_2(\alpha)$	1.6–2.2 (m)				
	$CH_2(\beta)$	1.2–1.4 (m)				
22	1,4	2.85 (m)	2136 [f]	51.9	51.5	56–57
	2,3	4.97 (m)	1986	4.91	4.72	
	CH_2	1.3–1.8 (m)	1940	5.99	6.00	
	MeNC	1.90 (s)				
23	1,4	2.70 (m)	2136 [f]	53.4	53.4	45–46
	2,3	4.95 (m)	1986	5.17	5.26	
	$CH_2(\alpha)$	1.6–2.1 (m)	1940	5.60	5.67	
	$CH_2(\beta)$	1.2–1.4 (m)				
	MeNC	1.91 (s)				
24	1,4	2.84 (m)	2126 [f]	53.1	53.4	50 °C/0.1 mmHg
	2,3	4.98 (m)	1984	5.08	5.26	
	CH_2	1.3–1.8 (m)	1938	5.18	5.67	
	EtNC	0.43 (t)				
		2.37 (q, $s = 7.4$)				
25	1,4	2.71 (m)	2124 [f]	55.7	55.2	50 °C/0.1 mmHg
	2,3	4.98 (m)	1982	5.67	5.75	
	$CH_2(\alpha)$	1.6–2.0 (m)	1938	5.45	5.36	
	$CH_2(\beta)$	1.2–1.4 (m)				
	EtNC	0.46 (t)				
		2.40 (q, $J = 7.4$)				
26	1,4	2.84 (m)	2122 [f]	56.8	56.7	49–50
	2,3	4.96 (m)	1986	6.15	6.18	
	CH_2	1.4–1.8 (m)	1938	5.01	5.09	
	Bu^{t}NC	0.77 (s)				
27	1,4	2.68 (m)	2144 [f]	58.1	58.1	88–89
	2,3	4.94 (m)	1982	6.18	6.57	
	$CH_2(\alpha)$	1.6–2.0 (m)	1926	4.90	4.84	
	$CH_2(\beta)$	1.2–1.4 (m)				
	Bu^{t}NC	0.79 (s)				

(continued)

Table 2 (continued)

Complex	^{1}H NMR		Infrared (cm^{-1})	Analysis		
				CHN (found)	CHN (calc)	M.p. (°C)
28	1,4	2.90 (m)	1991	43.9	43.7	60°C/0.1 mmHg
	2,3	4.86 (m)	1934	5.83	5.76	
	$CH_2(\alpha)$	1.6–2.0 (m)				
	$CH_2(\beta)$	1.2–1.4 (m)				
	$P(OMe)_3$	3.20 (d, 11.5)				
29	1,4	2.86 (m)	1994	63.2	62.8	87–88
	2,3	4.82 (m)	1942	4.91	4.84	
	$CH_2(\alpha)$	1.6–2.0 (m)				
	$CH_2(\beta)$	1.2–1.4 (m)				
	$P(OPh)_3$	7.1–7.5 (m)				

[a] C_6D_6 solution; H*a* = inner terminal diene proton; H*s* = outer terminal diene proton; values for tricarbonyl in square brackets. [b] Hexane solution. [c] from reference 8g. [d] 6.9–7.7 (m); other complexes are similar. [d] Under PPh_3. [f] CN vibration. [g] 270 MHz; other spectra at 100 MHz.

on the basis of modelling studies), though ^{31}P spectra show the presence of a second conformer which may be **A** or **B′**, but is arbitrarily assigned to **A** in Table 1. The ^{13}C spectra of the *cis*-pentadiene complex **3** (Fig. 1) show clearly two axial/basal pairs, consistent with population of only **B** and **B′**; the spectra do not distinguish between them, though **B** is arbitrarily assigned as the major conformer in Table 1. Conformer interconversion results in a^2/b^3 and a^1/b^4 exchange to give the two expected averaged resonances.

^{13}C spectra of the symmetric complexes **4** and **9** show a single, temperature invariant resonance consistent with exclusive population of the axial conformer, though the ^{31}P spectrum of the hexadiene complex shows that the **B**/**B′** enantiomer pair has a small population. The spectra of (cycloheptadiene)$Fe(CO)_2PPh_3$ (**21**) (Fig. 1) are as expected for a symmetrical complex populated exclusively by the basal conformer, showing a single, temperature invariant ^{31}P resonance and in the

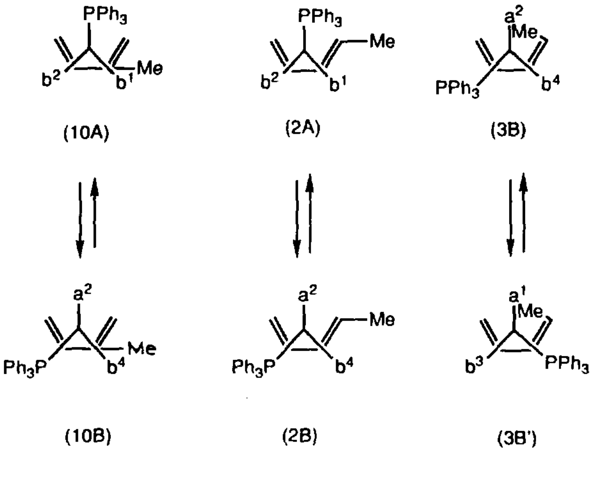

(10A) (2A) (3B)

(10B) (2B) (3B′)

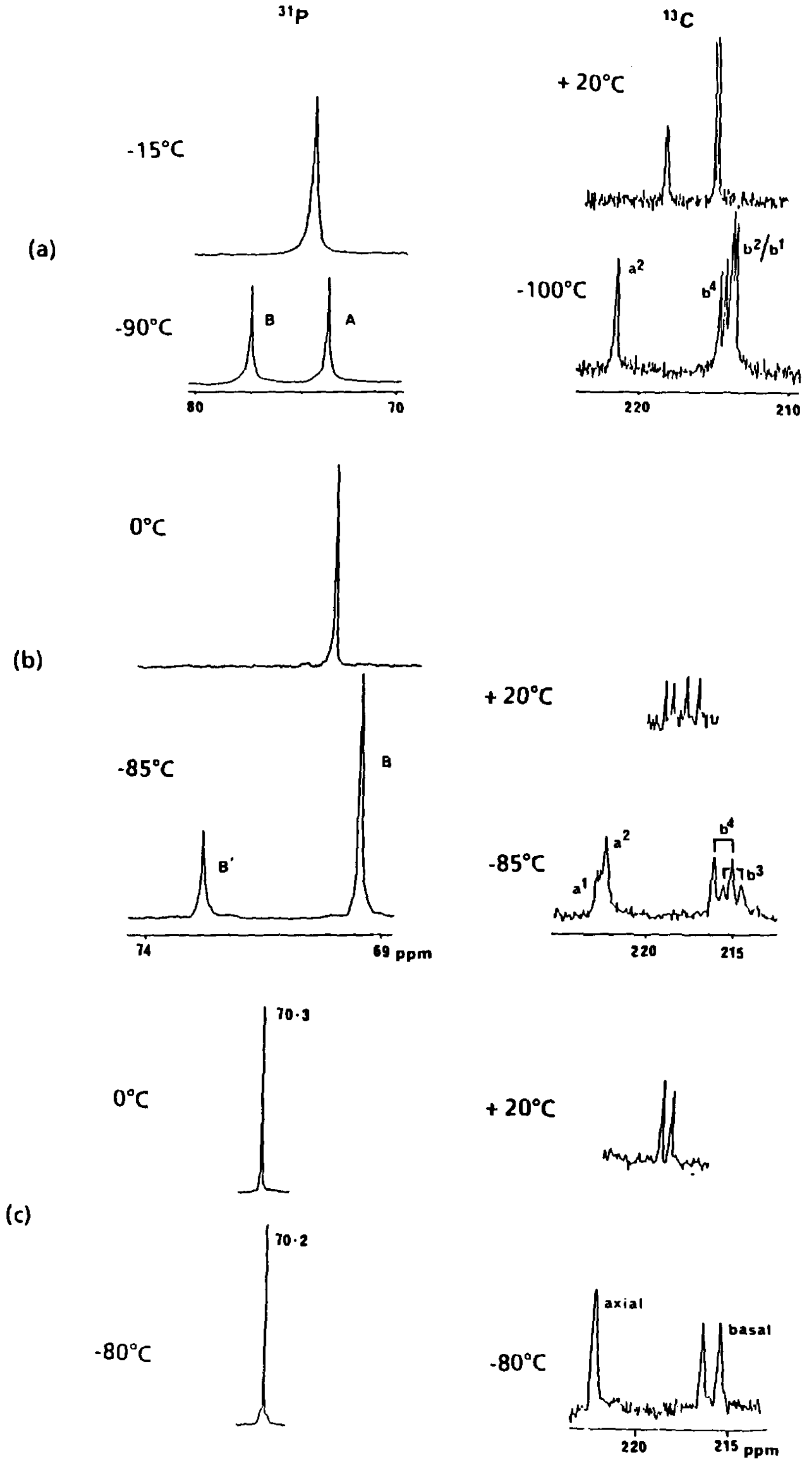

Fig. 1. High and low temperature ^{13}C and ^{31}P spectra of (a) (isoprene)$Fe(CO)_2PPh_3$, (b) (*cis*-pentadiene)$Fe(CO)_2PPh_3$, and (c) (cycloheptadiene)$Fe(CO)_2PPh_3$.

^{13}C spectrum, one axial/basal pair at low temperature which is averaged to a single resonance at high temperature. The cyclohexadiene complex **20** exhibits a temperature invariant ^{13}C spectrum down to $-90\,^{\circ}C$ due to a decreased rotational barrier, but the chemical shift and coupling constant of the averaged resonance are consistent with population of the basal conformer only, the conformer which is also observed in the solid state [14]. The changes in the ^{13}C spectrum of the butadiene complex **1** resemble those of the cycloheptadiene complex **21**, though the ^{31}P spectra show a significant population of the **B**/**B′** pair. Changes consistent with these exchange equilibria are also observed in the diene/alkyl region of all of the ^{13}C spectra.

The effects of alkyl substitution may be summarized as follows, taking the unsubstituted (butadiene)$Fe(CO)_2PPh_3$ as reference:

(a) *cis*-terminal substitution (as in **3**, **20** and **21**) depopulates completely the axial conformer.

(b) terminal or internal disubstitution (as in **4** and **9**) depopulates the basal conformer.

(c) *trans*-terminal monosubstitution depopulates the axial conformer while internal monosubstitution depopulates the basal isomer.

(d) in the isoprene series, methyl substitution of the phosphine increases the population of the axial conformer in the order $PPh_3 < PPh_2Me < PPhMe_2$. In all cases, the basal conformer is assigned to **B** rather than **B′** structure.

(iii) Single crystal and modelling studies of phosphine complexes

In order to confirm the solution NMR studies, and to provide a basis for the modelling studies, the structures of the hexadiene and 2,3-dimethylbutadiene complexes **4** and **9** have been determined by single crystal X-ray diffraction. The results (Table 3, Fig. 2) confirm the axial orientation of the PPh_3 ligand. Relative to the structure of (butadiene)$Fe(CO)_3$ [16], the main structural change is manifested in an increase in the axial ligand–Fe–diene angle (P/C_a–Fe–Z) coupled with a decrease in CO–Fe–CO basal angle. As with (cyclohexadiene)$Fe(CO)_2PPh_3$ [14], the steric effect of the phosphine appears to affect more its attitude relative to the diene rather than the CO ligands. In the hexadiene complex **4**, the two terminal methyls are twisted out of the diene plane towards the iron by an average of 3.5°, though this has been set to zero in the modelling studies. The Fe–P bond lengths and internal bond lengths and angles in the PPh_3 ligand are common to other (diene)$Fe(CO)_2PPh_3$ structures, all of which contain PPh_3 in a basal position [4c,14,16a–d].

Though full molecular mechanics calculations on transition metal complexes remain rare due to a lack of metal parameterization, recent results [17a–d] show that calculation of simple interligand Van der Waals interactions can provide an accurate estimate of relative conformer stabilities. Using CHEM-X [18], we have applied this approach to evaluate steric contributions to the relative stabilities of axial/basal conformers of the (diene)$Fe(CO)_2L$ series.

Though some of the gross features of the rotational profiles in Fig. 3 can be generated by rotation of the diene relative to a rigid $Fe(CO)_2PPh_3$ fragment using structures generated from the crystallographic coordinates, the more subtle features emerge only if

Table 3

Structural parameters for complexes **4**, **9**, **20** and **30**

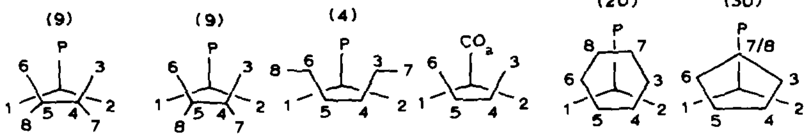

	(experimental)	(idealized)	(experimental)	(reference 15)	(idealized) [a]	(idealized)
Fe–C3	2.109(11)	2.109	2.149(5)	2.143	2.118	2.126
Fe–C4	2.065(11)	2.070	2.047(5)	2.058	2.060	2.060
Fe–C5	2.076(11)	2.070	2.056(4)	2.058	2.060	2.060
Fe–C6	2.106(11)	2.109	2.144(4)	2.143	2.118	2.126
Fe–Z [b]	1.68	1.68	1.68	1.67	1.69	1.74
C3–C4	1.426(15)	1.44	1.419(6)	1.45	1.42	1.42
C5–C6	1.453(14)	1.44	1.419(6)	1.45	1.42	1.42
C4–C5	1.362(13)	1.36	1.402(6)	1.45	1.42	1.42
C5/6–C8	1.523(15)	1.52	1.511(6)	–	1.53	1.52
C4/3–C7	1.513(15)	1.52	1.518(7)	–	1.53	1.52
C3–C4–C5	119(1)	117.4	118.6(4)	118.4	114.9	106.9
C6–C5–C4	116(1)	117.4	118.2(4)	118.4	114.9	106.9
C6–C5–C8	118(1)	118.9	–	–	–	–
C3–C4–C7	119(1)	118.9	–	–	–	–
C8–C6–C5	–	–	118.3(4)	–	120.2	107.8
C7–C3–C4	–	–	117.9(4)	–	120.2	107.8
C3–C4–C5–C6	0	0	–1.0	0	0	0
C7–C4–C5–C8	–1.3	0	–	–	–	–
C8–C6–C5–C4	–	–	–174.4	–	43.9	24.7
C7–C3–C4–C5	–	–	173.5	–	–43.9	–24.7
Fe–C1	1.689(11)	1.71	1.759(5)	1.77	1.76	1.76
Fe–C2	1.722(13)	1.71	1.755(5)	1.77	1.76	1.76
C1–O1	1.119(11)	1.18	1.152(6)	1.13	1.15	1.15
C2–O2	1.166(13)	1.18	1.150(5)	1.13	1.15	1.15
Ca–Oa	–	–	–	1.18	–	–
Fe–C1–O1	176(1)	180	174.9(4)	177.9	180	180
Fe–C2–O2	179(1)	180	178.0(4)	177.9	180	–
Fe–Ca–Oa	–	–	–	179.1	–	–
Fe–P/Ca	2.230(3)	2.23	2.236(1)	1.74	2.23	2.21
P–C9	1.826(10)	1.83	1.843(4)	–	1.84	1.83
P–C15	1.836(9)	1.83	1.838(4)	–	1.84	1.83
P–C21	1.822(10)	1.83	1.841(4)	–	1.84	1.83
C9–P–C15	99.4(4)	102.3	101.5(2)	–	102.2	102.7
C9–P–C21	103.2(4)	102.3	103.3(2)	–	102.2	102.7
C15–P–C21	103.7(4)	102.3	101.3(2)	–	102.2	102.7
Fe–P–C9	116.8(3)	115.6	115.9(1)	–	116.0	115.6
Fe–P–C15	116.7(3)	115.6	119.2(1)	–	116.0	115.6
Fe–P–C21	114.4(3)	115.6	113.3(1)	–	116.0	115.6
P/Ca–Fe–C1	101.1(4)	100.4	105.3(1)	101.8	101.3	101.3
P/Ca–Fe–C2	99.8(4)	100.4	101.8(1)	101.8	101.3	101.3
C1–Fe–C2	91.1(5)	91.0	88.6(2)	92.6	91.2	91.7
P/Ca–Fe–Z	118.8	118.8	116.4	114.1	117.8	117.8
Z–Fe–C1	120.5	120.4	119.2	121.2	120.2	120.2
Z–Fe–C2	120.3	120.4	121.0	121.2	120.2	120.2
C–C (ring)	1.390(14) (average)	1.39	1.387(7) (average)	–	1.39	1.39

[a] Other values: C7–C8 = 1.53, C6–C8–C7 = 110.7, C6–C8–C7–C3 = 0. [b] Z is the centroid of the C diene moiety.

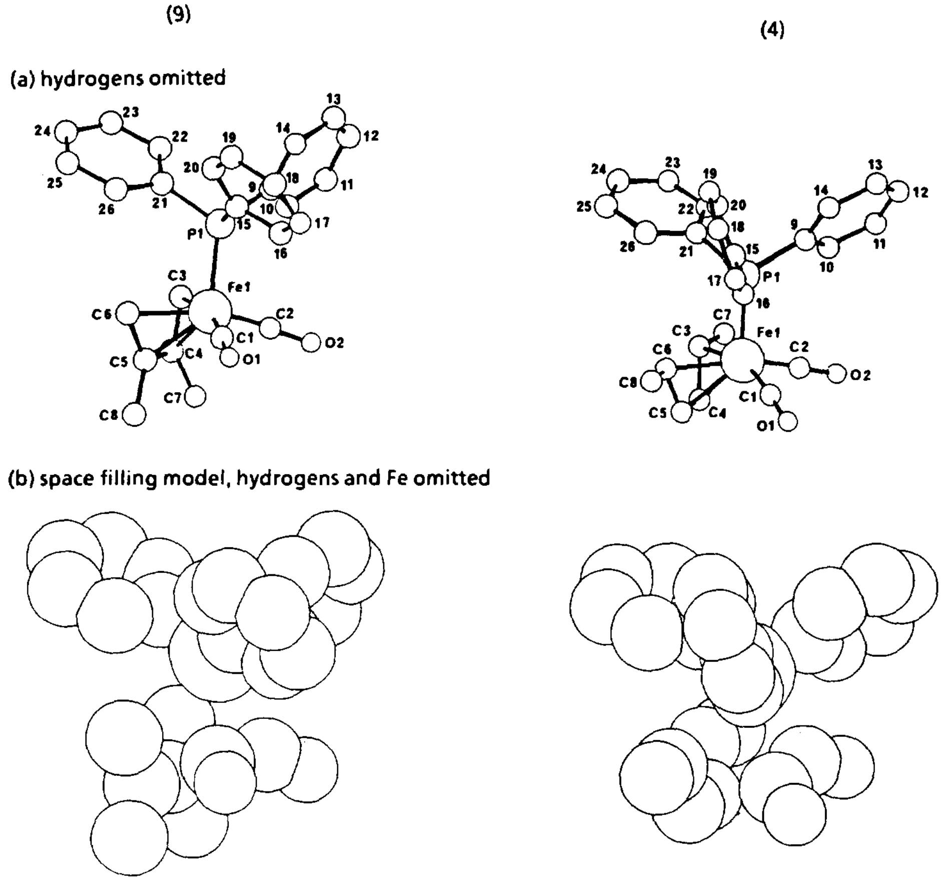

Fig. 2. Molecular structures of **4** and **9**.

(a) the molecular geometry is idealized [19] through equalization of symmetry related bond lengths and angles with the diene, within the PPh_3 ligand and within the square pyramidal polyhedron in symmetric complexes such as **9**. To isolate the effect of changes in the diene or metal substituent, all acyclic complexes were generated by modification of the idealized structure of **9**, thus retaining a constant PPh_3 and constant bond lengths and angles within the diene and the square pyramid. For the idealized cyclohexa- and cyclopentadiene complexes **20** and **30**, bond lengths and angles for the (diene)Fe moiety were taken from the basal literature structures [14,16c] but for consistency, superposed on an axial $Fe(CO)_2PPh_3$ fragment for the purposes of modelling.

(b) energy minimization about conformationally mobile Fe–P, P–C and C–C bonds is allowed. In particular, for symmetric complexes such as **4**, **9** or **20**, P–C minimization is necessary to generate isoenergetic profiles for the enantiomerically related clockwise/anticlockwise rotation of the diene relative to $Fe(CO)_2L$. The implication is that, as in the case of PPh_3 complexes chiral at iron [20], the screw sense of the PPh_3 propeller is linked to the molecular chirality. For asymmetric,

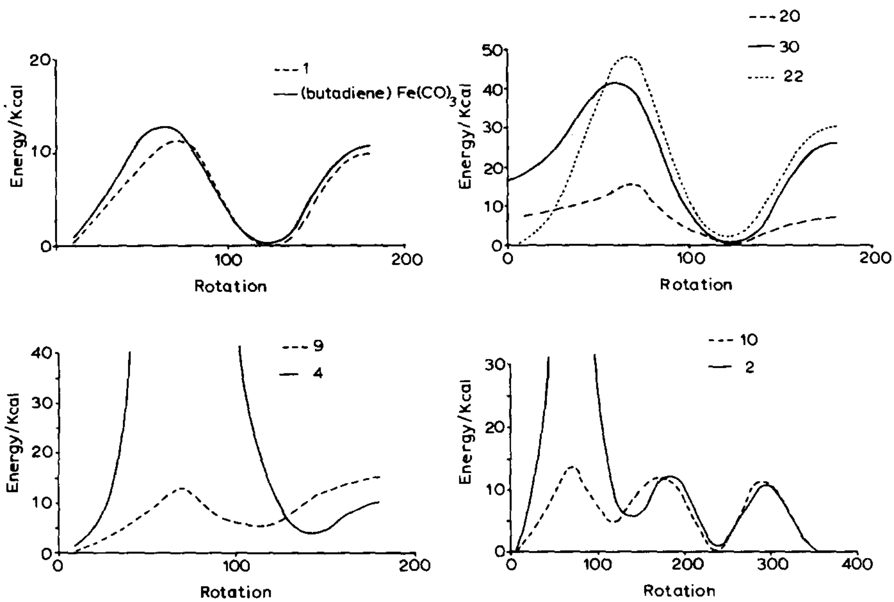

Fig. 3. Rotational energy profiles.

chiral complexes such as **3** and **10**, both enantiomers were generated and provided isoenergetic rotational profiles.

It may also be noted that axial/basal exchange requires not only turnstile rotation but also small changes in bond angle. As shown for (butadiene)$Fe(CO)_3$ in Fig. 3, neglect of bond angle change during rotation results in slightly unequal energy maxima at 60 and 180°, and a small overestimate of the energy of the equivalent ground state structure generated on 120° rotation. These inequalities disappear if all Z–Fe–CO and CO–Fe–CO angles are equalized. In Fig. 3, relative energies are plotted as a function of rotation, where 0° represents the axial isomer and rotation of the $Fe(CO)_2L$ fragment relative to the diene is clockwise. For symmetric complexes, only half of the symmetry related 360° rotation is shown. Since our interest is primarily in relative ground state energies, we have neglected bond angle changes during the turnstile rotation, though because of this small uncertainty (shown also by other tricarbonyls), we have deemed isoenergetic any conformer pair which differs in energy by less than two kcal.

Rotational profiles for the symmetric 2,3-dimethylbutadiene and hexadiene complexes **9** and **4** show clearly an enhanced stability of the axial PPh_3 conformer by about 5 kcal, in agreement with experiment. Profiles for the cyclic complexes **20** and **30** show in contrast an enhanced stability of the basal conformer by approximately 15 and 7 kcal respectively, again in agreement with experiment. Though we have yet to model the *cis*-pentadiene and cycloheptadiene complexes **3** and **21** [21*], a similar destabilization of the axial position is anticipated. It is interesting to note that in contrast to **9**, the *o*-xylylene complex **31** adopts the basal conformation in the solid state [16b]. Modelling of **31** reveals that the planarity of the *o*-xylylene unit is now sufficient to render the axial and basal positions isoenergetic in terms of steric interactions.

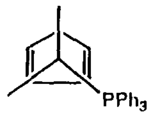

(30)

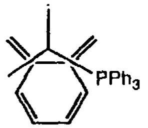

(31)

More subtle is the variation in conformer population between **1**, **2** and **10**. Modelling of the butadiene complex **1** shows no energy difference between axial and basal PPh_3 site occupancy; modelling of both the *trans*-pentadiene complex **2** and the isoprene complex **10** shows a destabilization of approximately 5 kcal for the basal site *cis* to the methyl, but no energy difference between the axial and the remaining unhindered basal site *trans* to methyl. Observance of only two populated conformers for **2** and **10** is thus consistent with these predictions; variation of the axial/basal ratio, which shifts towards basal on terminal substitution but towards axial on internal substitution, may be the result of electronic fine tuning. Both ^{13}C NMR [23a–c] and photoelectron spectra [24] show that the electronic effects of terminal versus internal methyl substitution are different. Most relevant are infrared force constant studies [9a], which show that though all methyl substituted dienes are net electron donors compared to butadiene, the increased back donation to axial and basal sites is not equal, and depends on the position of diene substitution. For (isoprene)$Fe(CO)_3$, the greatest relative change occurs in the basal force constant, implying a relatively greater back donation to the basal sites compared to (butadiene)$Fe(CO)_3$. Thus, in the more electron rich (isoprene)$Fe(CO)_2PPh_3$, a shift towards the axial PPh_3 conformer increases the basal site occupancy by the stronger π-accepting CO ligands. Conversely, terminal substitution (*cis* or *trans*) results in a greater and more pronounced relative change in the axial force constant. A shift towards the basal PPh_3 conformer thus maximizes axial site occupancy by CO. This appears also to be reflected in the ordering of the ^{31}P chemical shifts, which is $P_{basal} > P_{axial}$ for internal substitution, but $P_{axial} > P_{basal}$ for terminal substitution and for (butadiene)$Fe(CO)_2PPh_3$.

The observed shift towards axial conformer in the (isoprene)$Fe(CO)_2PPh_{3-x}Me_x$ series ($x = 0$–2) **10**–**12** as phosphine basicity increases [25] is also consistent with maximization of basal π-acceptance by CO. Though the effect may be partially steric, modelling studies of complexes **10**–**12** show no difference in energy between the **A** and **B** conformers. Though **B′** increases in relative stability, reflecting the decreasing cone angle [$PPh_3(145) > PPh_2Me(136) > PPhMe_2(122°)$], even for the $PPhMe_2$ complex, **B′** remains approximately 3 kcal higher in energy than the **A**/**B** pair.

The phenylbutadiene complex **5** provides a link between η^4-diene complexes and η^4-enone complexes of structure **32** which we have reported in a previous study [11a].

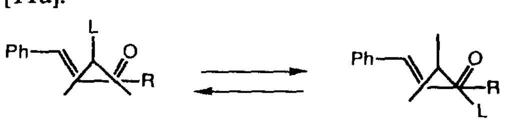

(A) (B)

(32a) R = H, L = PPh_3
b) R = H, L = PPh_2Me
c) R = H, L = $PPhMe_2$
d) R = Me, L = PPh_3

Though both **5** and **32a** show the presence of only conformers A and **B** in solution, there is a significant shift towards the axial conformer (for **5**, **A** : **B** = 1 : 13, for **32a**, **A** : **B** = 0.6 : 1). Modelling studies for both **5** and **32a** predict an isoenergetic **A/B** pair, with the **B′** conformer being > 10 kcal higher in energy for both complexes. The shift in conformer population thus seems a consequence of the stronger π-accepting character of the enone ligand. As in the isoprene series, there is an increase in axial conformer population for **32a–c** in the order $PPh_3 < PPh_2Me < PPhMe_2$. Introduction of a methyl group in **32d** also results in increased axial population (**A** : **B** = 59 : 1); and modelling studies of **32d** reveal an increase in the energy of **B** relative to **A** by approximately 4 kcal, with **B′** remaining > 10 kcal higher in energy.

We have not investigated in detail the dependence of total intramolecular energy on the orientation of the phenyl groups of the PPh_3 ligand relative to the diene along the Fe–P axis. One feature which seems to emerge is that in the higher energy areas of the energy profiles in Fig. 3, this orientation has a large influence on determining the energy minima, whereas at energies close to relative zero, the energy profiles with repect to Fe–P bond rotation are much flatter. The axial conformer of (cyclohexadiene)$Fe(CO)_2PPh_3$ (**20**) is an example of the former, with well defined minima at structures **33** and **34** (the latter slightly lower in energy) in which an approximate mirror plane bisects the CH_2–CH_2 bond. The energy maximum occurs at **35** in which CH_2 is directly eclipsed by a phenyl ring.

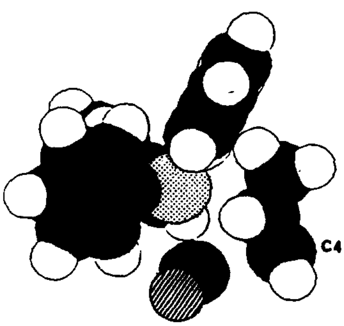

(33)

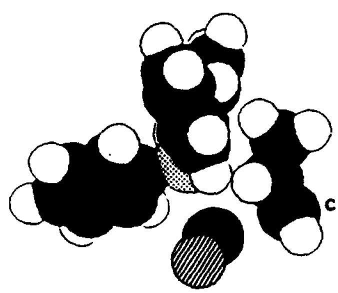

(34)

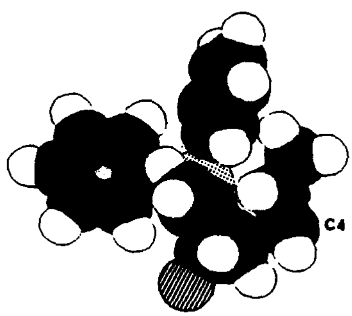

(35)

P
O
viewed down C4 - C5;
Fe omitted

The results raise the possibility of a concerted, cogwheel rotation in some of these complexes, a possibility we are investigating with sterically more demanding phosphines.

(iv) Solution structure and modelling of phosphite, isonitrile, arsine and stibine complexes

For the (isoprene)$Fe(CO)_2L$ series **15–18** containing sterically less demanding trimethylphosphite (cone angle 107°) and isonitrile ligands, modelling studies indicate no energy difference between the **A**/**B**/**B′** conformer trio, and solution NMR studies show that three conformers are populated in all cases. The phosphite complex **18** shows three ^{31}P resonances at low temperature (Fig. 4), the two major conformers being axial and basal. Though the spectra do not differentiate between **B** and **B′**, the major conformer is assigned the **B** structure on the basis of results on the PPh_3 complex. The bis(phosphite) complex **19** shows two unequal sets of doublets, the major set being assignable to the axial/basal conformer **AB** on the basis of couplings observed in the ^{13}C spectrum. The minor resonances are assigned to the alternative axial/basal conformer **AB′**. The basal/basal conformer is not populated; the reason may be steric, with the larger axial–basal angle minimizing interligand repulsions. The ratio of **AB** : **AB′** is similar to the **B** : **B′** ratio observed for **18**. Turnstile rotation in **19** does not completely scramble the phosphite ligands, and two broadened ^{31}P resonances are observed at 20 °C, still below the high temperature limiting spectrum.

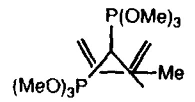

(19AB)

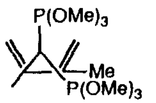

(19AB')

The cycloheptadiene complexes (**28**) and (**29**) show temperature invariant ^{31}P spectra which, in combination with axial/basal pair of resonances observed in the limiting low temperature ^{13}C spectra, indicate no detectable population of the axial phosphite conformer. Similar ^{31}P results have been reported for analogous iron complexes containing the cage phosphite $P(OCH_2)_3CEt$, though the ruthenium analogues do show some population of the axial conformer [8f].

^{13}C spectra of the isonitrile complexes, of which those of the CNEt derivatives **16** and **25** are typical (Fig. 4) show population of basal and axial conformers for both acyclic and cyclic complexes. All the cyclohexadiene and cycloheptadiene complexes exhibit a single CO resonance at 20 °C which is resolved at low temperature into an axial/basal pair due to the major basal CNR conformer and a single basal resonance due to the two symmetry related CO ligands of the axial CNR conformer. Two resonances which reflect the same conformer distribution are seen in the CN region at low temperature, though at room temperature the averaged CN resonance is broadened considerably by quadrupolar relaxation [26]. Our results on (cyclohexadiene)$Fe(CO)_2CNEt$ differ from those previously published [10c] where no axial CNEt conformer was detected, though axial/basal conformer mixtures have also been observed for (η^4-cyclooctatetraene)$Fe(CO)_2CNR$ derivatives [10d]. Spectra of the isoprene complexes are similar, though four rather than two basal CO resonances and three rather than two CN resonances are observed due to the inequivalence of the **B**/**B**′ conformer pair.

Compared to (isoprene)Fe(CO)$_2$PPh$_3$ (**10**), there is a shift of conformer population towards occupancy by phosphite or isonitrile of the better π-accepting basal site in the square pyramid [27], consistent with the accepted decreasing σ-donor/π-acceptor ratio of the ligand in the order PPh$_3$ > P(OMe)$_3$ > CO [25*]. The position of isonitrile is more problematical; photoelectron results on Fe(CO)$_4$CNR show that the isonitrile functions as a net electron acceptor, with π-acceptor and particularly σ-donor capacity reduced relative to CO; π-donor interactions may also play a role in the destabilization of the metal-centred orbitals [28]. This study also shows little variation in the electronic character of CNR as a function of R. The lower population of the axial isomer in the cycloheptadiene complexes **23**, **25** and **27**, compared to their cyclohexadiene analogues **22**, **24** and **26** and the increasing asymmetry in the **B**/**B**′ population of the isoprene complexes **15**–**17** may have a steric origin. Observations whose explanations remain unclear are the increased population of basal conformer in the isoprene series in the order CNMe < CNEt < CNBu^t and the increased population of what is expected to be the sterically more hindered axial isomer in the order CNMe < CNEt < CNBu^t for both the cyclohexadiene and cycloheptadiene complexes.

The origin of the shift in conformer population towards axial in the isoprene complexes **10**, **13** and **14** in the order PPh$_3$ < AsPh$_3$ < SbPh$_3$ is also unclear.

(v) Rotational barriers in (diene)Fe(CO)$_2$L complexes

Experimental rotational barriers for tricarbonyl complexes are in the range 9–13 kcal mol^{-1}, with a calculated electronic barrier for (butadiene)Fe(CO)$_3$ of 14.5 kcal mol^{-1} [13a]. We make no claim for the accuracy of the steric contribution to rotational barriers represented in Fig. 3, since they take no account of torsional or angular changes in the diene or polyhedron or movement of the iron relative to the diene at the transition state. Nevertheless, several features may be noted:

(a) in all cases, steric factors favour the staggered structure **36s** rather than the eclipsed **36e** as the ground state, thus reinforcing the electronic preference for the staggered geometry [29].

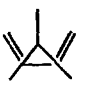
(36s)


(36e)

(b) in all cases except the pentadiene and hexadiene complexes **3** and **4**, energies of the eclipsed transition state for the Fe(CO)$_2$PPh$_3$ and Fe(CO)$_3$ complexes are close (as shown in Fig. 3 for (butadiene)Fe(CO)$_2$L), thus indicating that the large PPh$_3$ should not sterically influence rotational barriers. The pentadiene and hexadiene complexes show substantially larger barriers for passage of PPh$_3$ past the *trans*-terminal methyl group, reaching a maximum of ca. 80 kcal in each case at 70° rotation. There is no evidence for such a massively increased barrier for the axial/basal exchange in the variable temperature ^{31}P spectra of the hexadiene complex **4**. The possible reduction in energy of the 70° transition state was modelled via elongation along the Fe–Z axis or twisting about C5–C6 to move the terminal methyl further from the PPh$_3$. In both cases, the energy falls dramatically.

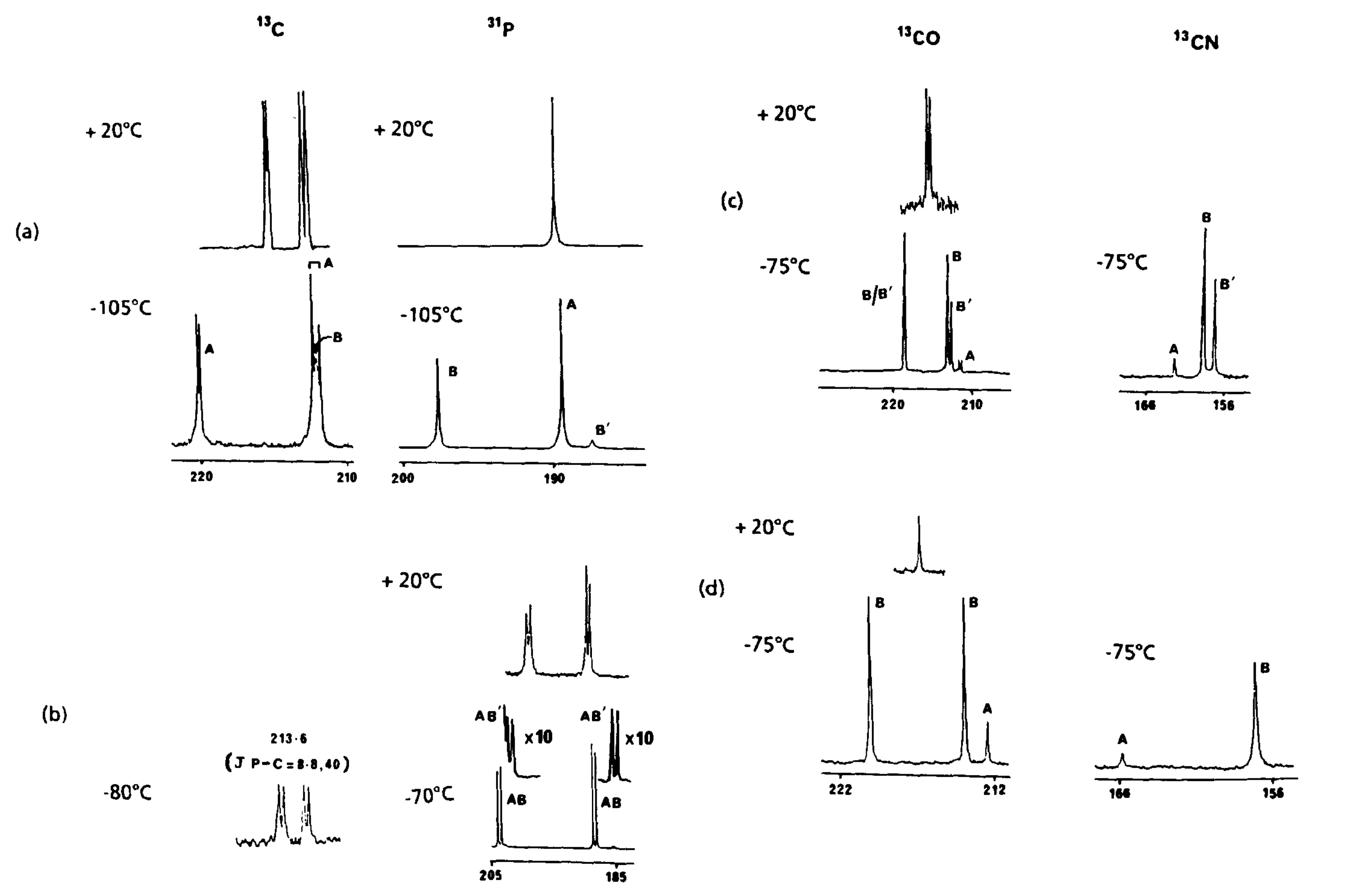

Fig. 4. ^{13}C and ^{31}P spectra of (a) (isoprene)$Fe(CO)_2P(OMe)_3$, (b) (isoprene)$Fe(CO)_2[P(OMe)_3]_2$, (c) (isoprene)$Fe(CO)_2CNet$ and (d) (cycloheptadiene)$Fe(CO)_2CNEt$.

Elongation along the Fe–Z axis such as to increase the Fe–C distances by ca. 0.3 Å or twisting of methyl away from the iron by ca. 35° both reduce the transition state to an energy comparable with other $Fe(CO)_2PPh_3$ and $Fe(CO)_3$ complexes. The energy cost of such distortions in terms of orbital overlap is unknown, though it may be noted that twisting angles larger than 35° are found in the ground state structures of C_6 and C_7 cyclic (diene)$Fe(CO)_3$ complexes. Energy profiles for the smaller isonitrile ligands are essentially superposable on those of the tricarbonyls, as shown for (cyclohexadiene)$Fe(CO)_2$CNMe in Fig. 3.

(c) Through line shape analysis of variable temperature ^{31}P and ^{13}C spectra [30*], we have determined rotational barriers for (isoprene)$Fe(CO)_2L$ of $\Delta H^{\star} = 6.8 \pm 0.1$ kcal mol^{-1}, $\Delta S^{\star} = -13.9 \pm 0.5$ cal K^{-1} mol^{-1} for L = PPh_3 and $\Delta H^{\star} = 9.8 \pm 0.5$ kcal mol^{-1}, $\Delta S^{\star} = -2 \pm 2$ cal K^{-1} mol^{-1} for L = CO. In common with other PPh_3 and PF_3 complexes [9a,b,11a], phosphine substitution thus appears to decrease the rotational barrier. The origins of this remain obscure, since calculations [13a] predict an increase in rotational barrier with increasing σ-donor capacity due to tilting changes in the $2e_s$ and $1e_s$ orbitals of the $Fe(CO)_3$ fragment which reduce the asymmetry in the important $2e_s$–π_3 (butadiene) and $1e_s$–π_3 (butadiene) orbital overlaps in the staggered and eclipsed configurations. Within the precision of such measurements, rotational barriers for $Fe(CO)_2$CNR [10a] and $Fe(CO)_3$ [8a] complexes are identical.

(vi) Restricted C–CHO rotation in (sorbaldehyde)$Fe(CO)_2L$ (L = CO, PPh_3, $P(OMe)_3$)

Introduction of an electron withdrawing substituent to a terminal diene carbon is known to substantially increase the barrier to rotation. In complexes such as **6–8** and their $Fe(CO)_3$ analogues the conjugative effect is maximized through coplanarity of the CHO or CO_2Me substituent, and for (sorbaldehyde)$Fe(CO)_3$, indirect evidence from protonation studies indicates an equally populated mixture of the *cis/trans* isomers **37** and **38** [31]. We here present direct NMR evidence for this rotational process.

Diene rotation in (sorbaldehyde)$Fe(CO)_3$ is slow on the NMR time scale at −60 °C, as evidenced by the well resolved axial/basal CO resonances (Fig. 5). Below −70 °C, all ^{13}C resonances (except the methyl) show additional broadening. Though a limiting low temperature spectrum cannot be obtained, that at −125 °C shows a clear splitting into unequally populated resonances of one of the basal CO resonances and the C-3 inner diene resonance. From modelling studies, the *cis/trans* forms of (sorbaldehyde)$Fe(CO)_3$ appear equal in energy; the experimentally observed asymmetry in the *cis/trans* distribution evident in the low temperature NMR spectrum is at most in the range 2–3 : 1.

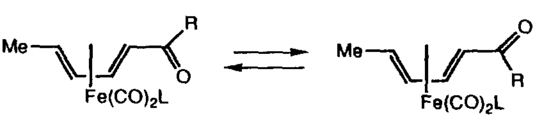

(37) cis (38) trans

L = CO, PPh_3, $P(OMe)_3$

R = H , OMe

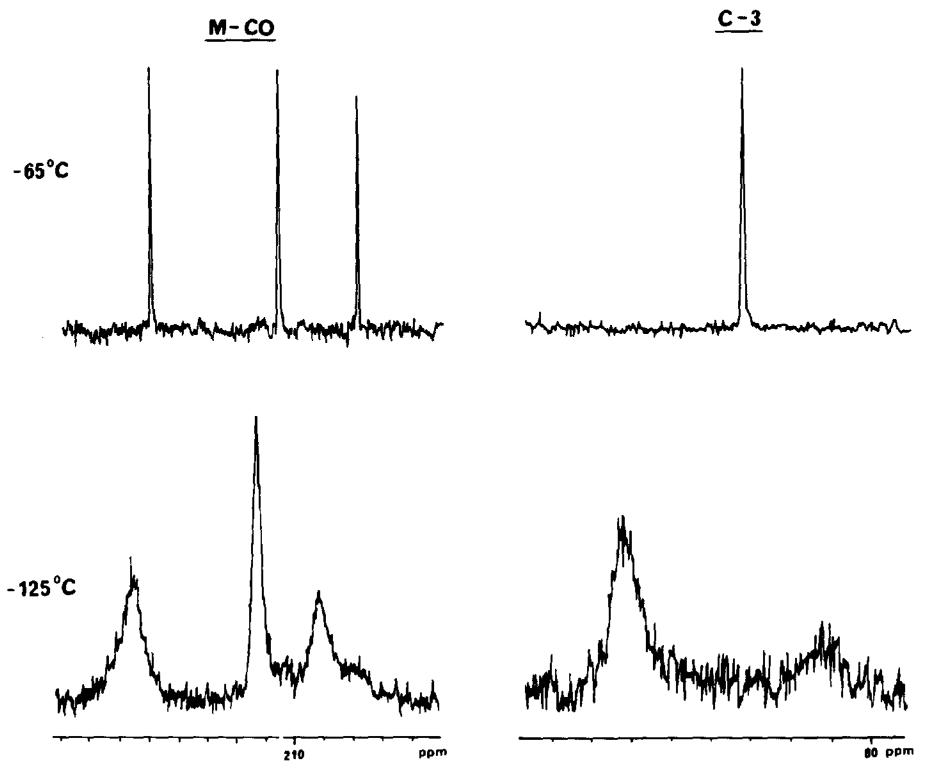

Fig. 5. ^{13}C spectra of sorbaldehyde $Fe(CO)_3$ (Et_2O-d^{10}).

^{31}P spectra of the sorbaldehyde complexes **7** and **8** both show features at low temperature (Fig. 6) which seem best explained by slowing of C–CHO bond rotation.

The ^{31}P spectrum of the PPh_3 complex **7** exhibits a singlet at 20 °C which is resolved into two resonances at -60 °C; on the basis of the ^{13}C NMR at this temperature which shows clearly a basal pair of resonances [32*], the major conformer contains axial PPh_3. Identification of the minor basal conformer as **B** or **B′** is not possible; though modelling studies show clearly a greater stability of the axial conformer by ca. 8 kcal, they do not distinguish between the two basal conformers. Below -60 °C, the resonance due to the axial conformer broadens again; the spectrum at -105 °C, though not quite low temperature limiting, exhibits two resonances of slightly unequal population. Modelling studies of the axial PPh_3 conformer indicate that the *cis* conformer **37** is more stable than **38** by ca. 3 kcal. The resonance due to the minor basal conformer remains sharp down to -105 °C, indicating that only **37** or **38** is populated. Modelling studies on both possible basal conformers indicate that **37** is more stable by > 10 kcal.

Both the ^{13}C and ^{31}P spectra of the methylsorbate complex **6** are essentially temperature invariant, indicating population of only the axial PPh_3 conformer and, most probably, only the *trans* conformer **38** based on the solid-state structure of (methylsorbate)$Fe(CO)_2PPh_2$(neomenthyl) [6a].

^{13}C and ^{31}P spectra of the $P(OMe)_3$ complex **8** (Fig. 5) resemble those of the PPh_3 complex **7** except that $P(OMe)_3$ exhibits a greater preference for basal occupation,

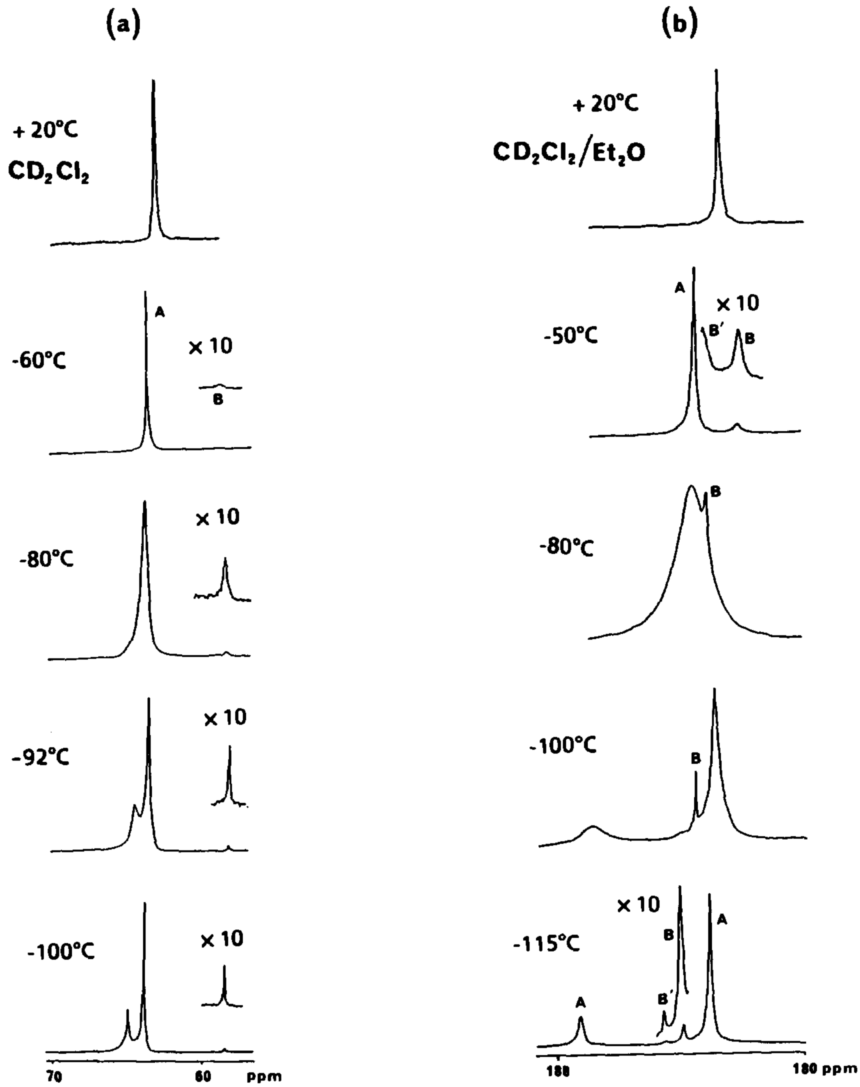

Fig. 6. Variable temperature ^{31}P spectra of (a) (sorbaldehyde)$Fe(CO)_2PPh_3$ and (b) (sorbaldehyde)-$Fe(CO)_2P(OMe)_3$.

and both basal conformers are populated, though unequally. On cooling to $-115°C$, resonances due to the axial and minor basal isomers exhibit changes attributable to slowing of C–CHO rotation, though due to overlap, only one of the resonances due to the minor basal isomer is apparent. Though a distinction between the two basal isomers is not possible on the basis of NMR or modelling data, the resonance due to the major basal isomer remains sharp down to $-115°C$, indicating, as in the PPh_3 case, probable population of only the *cis* conformer **37**.

The ability of auxiliary ligands to control the *cis*/*trans* ratio may provide an important influence on the diastereoselectivity of reactions at the aldehydic carbon, which are important in the synthetic utility of these complexes [2].

Experimental

All reactions were performed under nitrogen using distilled and degassed solvents. NMR spectra were recorded on JEOL FX-100 or JEOL GSX-270 spectrometers; infrared spectra were recorded on a Pye Unicam SP2000 spectrometer. *trans*-1-Phenyl-1,3-butadiene [34], and the isonitrile ligands [35] were prepared by literature methods. With the exception of (butadiene)Fe$(CO)_3$ which was purchased, all (diene)Fe$(CO)_3$ complexes were prepared by ultrasonic reaction of the diene with $Fe_2(CO)_9$ [36].

*(a) Preparation of (isoprene)Fe$(CO)_2PPh_3$ (**10**)*

$Me_3NO \cdot 2H_2O$ (7.7 g, 68.8 mmol) was added to a stirred solution of (isoprene)Fe$(CO)_3$ (8 g, 38.4 mmol) and PPh_3 (16 g, 61.1 mmol) in acetone (150 ml). The mixture was vigorously stirred at reflux until infrared sampling indicated disappearance of starting material. Diethyl ether (200 ml) was added to the cooled mixture which was filtered and evaporated. The residue was dissolved in diethyl ether (75 ml) and stirred with excess MeI for one hour to remove unreacted PPh_3. After filtration and removal of solvent the residue was extracted with 10% ethyl acetate/petroleum ether (30–40) and chromatographed on alumina using 5% ethyl acetate/petroleum ether (30–40). Evaporation of solvent from the yellow band collected gave the product **10**, as a yellow solid (10.6 g, 55%). An analytical sample was obtained by crystallization from petroleum ether (30–40).

Other PPh_3 complexes and the PPh_2Me, $PPhMe_2$, $AsPh_3$, $SbPh_3$ and isonitrile complexes were prepared in the same way; analytical samples were obtained either by crystallization from petroleum ether (30–40) or in the case of oils, microdistillation at the temperatures and pressures shown in Table 2.

(b) Preparation of (isoprene)Fe$(CO)_x[P(OMe)_3]_{3-x}$ (x = 1, 2)

(i) (isoprene)Fe$(CO)_3$ (3 g, 14.4 mmol) and $P(OMe)_3$ (2 g, 16.1 mmol) were stirred in toluene (600 ml) and irradiated using a 90W medium pressure Hg lamp until infrared sampling indicated almost complete disappearance of starting material. After removal of solvent, the crude product was purified by preparative tlc on silica using 3% ethyl acetate/petroleum ether (30–40). The product was collected as the main yellow band which separated from traces of the faster moving tricarbonyl and the slower moving disubstituted complex. Extraction and microdistillation provided **18** (1.5 g, 35%).

(ii) (isoprene)Fe$(CO)_3$ (2 g, 9.6 mmol) and $P(OMe)_3$ (4 g, 32.2 mmol) were stirred and irradiated in toluene (600 ml) with further additions of phosphite until infrared sampling indicated complete disappearance of the monosubstituted complex **18**. After removal of solvent, the residue was purified by preparative tlc on silica using 3% ethyl acetate/petroleum ether (30–40). Collection of the faster moving yellow band, followed by extraction and microdistillation yielded **19** (650 mg, 17%). The slower moving yellow band was identified by NMR as the fully substituted (isoprene)Fe$[P(OMe)_3]_3$ complex [37a,b].

Complexes **28** and **29** were prepared by reaction of (cycloheptadiene)Fe$(CO)_3$ with phosphite in di-n-butylether [5a].

*(c) Crystallographic data for complexes **4** and **9***

Data were collected on a Hilger Watts Y290 diffractometer using Mo-K_α radia-

Table 4

Details of data collection for compounds **4** and **9**

	4	**9**
	$C_{26}H_{25}O_2PFe$	$C_{26}H_{25}O_2PFe$
	triclinic	monoclinic
space group	$P\bar{1}$	$P2_1/c$
Z	2	4 (two molecules per lattice point).
a (Å)	10.492(3)	10.297(3)
b (Å)	10.263(2)	28.782(6)
c (Å)	11.623(2)	15.708(5)
α (°)	77.21(2)	90
β (°)	84.00(2)	98.99(2)
γ (°)	67.68(2)	90
U (Å^3)	1128.78	4598.1
μ (cm^{-1})	18.55	18.22
F(000)	476	1908
range	$2 < \theta < 28$	$2 < \theta < 24$
reflections $I > 3\sigma(I)$	3115	3124
variable parameters	151	272
maximum shift/esd	< 0.001	< 0.001
R	5.55%	6.88
R_w	6.67	7.17
maximum excursion	0.29 e/Å^3	0.18 e/Å^3
minimum excursion	−0.21	−0.19

tion (0.71069 Å). Structures were solved by a combination of Patterson search and direct methods (SHELX86) [38] and refined by full matrix least squares (SHELX76) [39]. Data were corrected for Lorentz and polarization effects, but not for absorption. Hydrogen atoms were included in calculated positions. For **4**, the iron, phosphorus and carbonyl groups were refined anisotropically; for **9**, only iron and phosphorus were refined anisotropically. Atomic scattering factors for hydrogen and non-hydrogen atoms and the anomalous dispersion correction factors for non-hydrogen atoms were taken from the literature [40–42]. Calculations were performed on a VAX 11/785 computer. Tables of calculated and observed structure factors and anisotropic and isotropic thermal parameters are available from the authors as supplementary material. Atomic coordinates are listed in Table 5.

For complex **9**, there are two independent molecules per lattice point, but bond length differences between the two are close to experimental error and are not considered chemically significant.

(d) Molecular modelling studies

The idealized structure of (2,3-dimethylbutadiene)Fe$(CO)_2PPh_3$ (**9**) (Table 3) was generated by modification of the experimentally determined structure, and all acyclic (diene)Fe$(CO)_2$L and (η^4-enone)Fe$(CO)_2$L complexes were generated from this by changing the substitution of the diene or alteration of L. Idealized diene geometries for **20** and **30** were generated from literature structures of **20** [14] and (5-*exo*-benzyl-1,3-cyclopentadiene)Fe$(CO)_2PPh_3$ [16c], but the Fe$(CO)_2PPh_3$ moiety was altered such that PPh_3 occupied an axial position. The Fe$(CO)_3$ complexes were generated from Fe$(CO)_2PPh_3$ by replacement of PPh_3 with a linear CO having

Table 5

Fractional atomic coordinates for complexes **4** and **9**

Atom	*x*	*y*	*z*
Complex 4			
Fe1	0.06858(5)	0.14392(5)	0.15149(5)
P1	0.20248(10)	0.13168(10)	0.29412(8)
O1	−0.1627(4)	0.0716(4)	0.2656(4)
O2	0.1863(4)	−0.1447(4)	0.1028(4)
C1	−0.0690(5)	0.0998(5)	0.2254(4)
C2	0.1420(5)	−0.0307(5)	0.1227(4)
C7	0.3090(5)	0.1254(6)	−0.0511(5)
C3	0.1860(4)	0.2223(5)	0.0099(4)
C4	0.0524(5)	0.2420(5)	−0.0229(4)
C5	−0.0619(5)	0.3188(5)	0.0409(4)
C6	−0.0378(4)	0.3711(4)	0.1365(4)
C8	−0.1595(5)	0.4418(6)	0.2126(5)
C9	0.3267(4)	−0.0487(4)	0.3541(3)
C10	0.4025(4)	−0.1376(5)	0.2751(4)
C11	0.4945(5)	−0.2758(5)	0.3159(5)
C12	0.5130(5)	−0.3275(6)	0.4362(5)
C13	0.4385(5)	−0.2426(6)	0.5148(5)
C14	0.3460(5)	−0.1027(5)	0.4737(4)
C15	0.1217(4)	0.1944(4)	0.4299(3)
C16	−0.0088(5)	0.1971(5)	0.4650(4)
C17	−0.0694(5)	0.2444(5)	0.5693(5)
C18	−0.0012(5)	0.2880(5)	0.6368(4)
C19	0.1310(6)	0.2831(6)	0.6044(5)
C20	0.1921(5)	0.2364(5)	0.5002(4)
C21	0.3120(4)	0.2388(4)	0.2467(3)
C22	0.4454(5)	0.1800(5)	0.2025(4)
C23	0.5189(6)	0.2673(6)	0.1547(5)
C24	0.4634(5)	0.4121(5)	0.1534(4)
C25	0.3318(5)	0.4719(6)	0.1975(4)
C26	0.2559(5)	0.3854(5)	0.2437(4)
Complex 9			
Fe1	0.58529(15)	0.11231(5)	0.93935(9)
Fe2	0.79780(14)	−0.07170(5)	1.44871(9)
P1	0.7522(3)	0.1089(1)	0.8646(2)
P2	0.7933(3)	−0.1412(1)	1.5070(2)
O1	0.3930(8)	0.1608(3)	0.8177(5)
O2	0.6406(10)	0.1961(4)	1.0393(6)
O3	1.0769(9)	−0.0562(3)	1.4973(5)
O4	0.7226(8)	−0.0083(3)	1.5773(5)
C1	0.4719(11)	0.1415(4)	0.8663(7)
C2	0.6218(12)	0.1615(4)	0.9968(8)
C3	0.6761(11)	0.0680(4)	1.0379(7)
C4	0.5402(11)	0.0747(4)	1.0428(7)
C5	0.4498(11)	0.0648(4)	0.9722(7)
C6	0.5014(11)	0.0480(4)	0.8968(7)
C7	0.5007(13)	0.0950(5)	1.1238(8)
C8	0.3017(12)	0.0714(4)	0.9649(8)
C9	0.9045(9)	0.1377(3)	0.9116(6)
C10	0.9355(11)	0.1437(4)	1.0004(7)
C11	1.0532(12)	0.1654(4)	1.0365(8)
C12	1.1373(12)	0.1815(4)	0.9851(7)

Table 5 (continued)

Atom	x	y	z
C13	1.1092(11)	0.1771(4)	0.8969(7)
C14	0.9940(10)	0.1546(4)	0.8612(7)
C15	0.7261(9)	0.1358(3)	0.7574(6)
C16	0.6838(10)	0.1820(3)	0.7534(6)
C17	0.6656(11)	0.2077(4)	0.6759(7)
C18	0.6923(11)	0.1862(4)	0.6032(8)
C19	0.7340(11)	0.1403(4)	0.6044(8)
C20	0.7518(10)	0.1154(4)	0.6825(6)
C21	0.8058(9)	0.0501(3)	0.8443(6)
C22	0.9244(10)	0.0319(3)	0.8913(6)
C23	0.9540(11)	−0.0152(4)	0.8825(7)
C24	0.8696(10)	−0.0433(4)	0.8290(6)
C25	0.7575(11)	−0.0265(4)	0.7817(7)
C26	0.7244(11)	0.0209(4)	0.7894(6)
C27	0.9631(12)	−0.0617(4)	1.4789(7)
C28	0.7524(10)	−0.0354(4)	1.5272(7)
C29	0.6057(12)	−0.0794(4)	1.3787(7)
C30	0.6705(10)	−0.0390(4)	1.3504(6)
C31	0.7931(10)	−0.0469(4)	1.3247(6)
C32	0.8374(12)	−0.0938(4)	1.3270(7)
C33	0.6150(12)	0.0097(4)	1.3556(8)
C34	0.8763(12)	−0.0080(4)	1.2966(8)
C35	0.6538(9)	−0.1587(3)	1.5603(6)
C36	0.5606(10)	−0.1260(4)	1.5772(6)
C37	0.4569(12)	−0.1397(4)	1.6191(7)
C38	0.4444(11)	−0.1846(4)	1.6435(7)
C39	0.5344(10)	−0.2165(4)	1.6256(6)
C40	0.6410(10)	−0.2049(3)	1.5857(6)
C41	0.9280(9)	−0.1550(3)	1.5950(6)
C42	0.9871(10)	−0.1992(3)	1.6061(6)
C43	1.0831(10)	−0.2077(4)	1.6774(6)
C44	1.1236(11)	−0.1740(4)	1.7354(7)
C45	1.0671(11)	−0.1301(4)	1.7255(7)
C46	0.9710(10)	−0.1211(4)	1.6562(6)
C47	0.8026(10)	−0.1882(3)	1.4309(6)
C48	0.9198(11)	−0.1961(4)	1.4011(6)
C49	0.9287(12)	−0.2287(4)	1.3369(7)
C50	0.8212(11)	−0.2529(4)	1.3024(7)
C51	0.7024(12)	−0.2456(4)	1.3282(7)
C52	0.6926(10)	−0.2125(3)	1.3926(6)

Fe–C and C–O bond lengths equal to the basal carbonyls; linear CNR ligands were introduced in the same way using Fe–C, C–N and N–R distances of 1.82, 1.15 and 1.55 Å respectively [10b]. The C–Ph and ketonic C=O bond lengths used for **5** and **32** were 1.46 and 1.32 Å [43]. The PPh_2Me and $PPhMe_2$ complexes were generated by sequential substitution of Ph by Me with no alteration in P–C distances or C–P–C angles [44]. The $P(OMe)_3$ complexes were modelled using an Fe–P distance of 2.13 Å [3c] and average internal ligand parameters taken from the structure of $Fe(CO)_2[P(OMe)_3]_3$ (P–O = 1.69, O–Me = 1.44 Å; O–P–O = 104.3, P–O–Me = 121.0°) [45]. For the rotational profiles in Fig. 3, Van der Waals energies were calculated using default parameters (including all atoms except iron) at 5° intervals with respect to rotation about the Fe–Z bond, allowing energy minimization with respect to rotation about Fe–P and other conformationally mobile bonds. Other $Fe(CO)_2L$ complexes were assessed for axial/basal energy differences only at 120 and 240° rotation angles.

References

1 For recent leading articles, see (a) A.J. Pearson, Philos. Trans. R. Soc. London, A, 326 (1988) 525; (b) A.J. Pearson, Adv. Met.-Org. Chem., 1 (1989) 1; (c) G.R. Stephenson, R.P. Alexander, C. Morley and P.W. Howard, Philos. Trans. R. Soc. London, A, 326 (1988) 545.

2 For recent review, see R. Gree, Synthesis, (1989) 341.

3 (a) A.J. Birch and L.F. Kelly, J. Organomet. Chem., 286 (1985) C5; (b) B.F.G. Johnson, J. Lewis, G.R. Stephenson and E.J.S. Vichi, J. Chem. Soc., Dalton Trans., (1978) 369; (c) C.M. Adams, A. Hafner, M. Koller, A. Marcuzzi, R. Preivo, I. Solana, B. Vincent and W. von Philipsborn, Helv. Chim. Acta, 72 (1989) 1658.

4 (a) A.J. Birch, W.D. Raverty, S.Y. Hsu and A.J. Pearson, J. Organomet. Chem., 260 (1984) C59; (b) J.A.S. Howell, M.C. Tirvengadum and G. Walton, J. Organomet. Chem., 338 (1988) 217; (c) J.A.S. Howell, A.D. Squibb, Z. Goldschmidt, H.E. Gottlieb, A. Almadhoun and I. Goldberg, Organometallics, 9 (1990) 80.

5 (a) A.J. Pearson, S.L. Kole and T. Ray, J. Am. Chem. Soc., 106 (1984) 6060; (b) A.J. Pearson and J. Yoon, Tetrahedron Lett., 26 (1985) 2399.

6 (a) J.A.S. Howell, M.C. Tirvengadum, A.D. Squibb, G. Walton, P. McArdle and D. Cunningham, J. Organomet. Chem., 347 (1988) C5; (b) J.A.S. Howell, A.D. Squibb, G. Walton, P. McArdle and D. Cunningham, ibid., 319 (1987) C45; (c) J.A.S. Howell and M.J. Thomas, J. Chem. Soc., Dalton Trans., (1983) 1401; (d) W.Y. Zhang, D.J. Jakiela, A. Maul, C. Knors, J.W. Lauher, P. Helquist and D. Enders, J. Am. Chem. Soc., 110 (1988) 4652.

7 For a preliminary communication of part of this work, see J.A.S. Howell and G. Walton, J. Chem. Soc., Chem. Commun., (1986) 622.

8 (a) P. Bischofberger and H.J. Hansen, Helv. Chim. Acta., 65 (1982) 721; (b) L. Kruczynski and J. Takats, Inorg. Chem., 15 (1976) 3140; (c) D. Leibfritz and H. tom Dieck, J. Organomet. Chem., 105 (1976) 255; (d) C.G. Kreiter, S. Stuber and L. Wackerle, ibid., 66 (1974) C49; (e) J.Y. Lallemand, P. Laszlo, C. Muzette and A. Stockis, ibid., 91 (1975) 71; (f) T.H. Whitesides and R.A. Budnik, Inorg. Chem., 14 (1975) 664; (g) S. Zobi-Ruh and W. von Philipsborn, Helv. Chim. Acta, 63 (1980) 773.

9 (a) M.A. Busch and R.J. Clark, Inorg. Chem., 14 (1975) 219, 226; (b) J.D. Warren and R.J. Clark, Inorg. Chem., 9 (1970) 373.

10 (a) M. Moll, H.J. Seibold and W. Popp, J. Organomet. Chem., 191 (1980) 193; (b) H. Behrens, G. Thiele, A. Purzer, P. Wurstl and M. Moll, ibid., 160 (1978) 255; (c) M. Moll, W. Popp and P. Wurstl, Z. Anorg. Allg. Chem., 516 (1984) 127, (d) M.J. Hails, B.E. Mann and C.M. Spencer, J. Chem. Soc., Dalton Trans., (1985) 693.

11 (a) J.A.S. Howell, D.T. Dixon and J.C. Kola, J. Organomet. Chem., 266 (1984) 69; (b) E.J.S. Vichi, F.Y. Fujiwara and E. Stein, Inorg. Chem., 24 (1985) 286.

12 Chemical shifts for the limiting low temperature spectrum of (isoprene)$Fe(CO)_3$ (-85 °C, toluene-d_8) are 210.4, 210.6 (basal) and 216.3 ppm (axial) giving a single averaged resonance at $+20$ °C of 211.8 ppm; These values are typical of cyclic and acyclic alkyl and aryl substituted complexes [8b,11a].

13 (a) T.A. Albright, P. Hofmann and R. Hoffmann, J. Am. Chem. Soc., 99 (1977) 7546; (b) D.J. Cole-Hamilton and G. Wilkinson, Nouv. J. Chim., 1 (1977) 141.

14 A.J. Pearson and P.R. Raithby, J. Chem. Soc., Dalton Trans., (1981) 884.

15 O.S. Mills and G. Robinson, Acta Cryst., 16 (1963) 758.

16 (a) D. Wormsbacher, F. Edelmann, D. Kaufmann, U. Behrens and A. de Meijere, Angew. Chem., Int. Ed. Engl., 20 (1981) 696; (b) R.E. Davis, personal communication; (c) G.A. Sim, D.I. Woodhouse and G.R. Knox, J. Chem. Soc., Dalton Trans., (1979) 629; (d) K.D. Karlin, M.P. Moiran, M. Kustyn, P.L. Dahlstrom, J. Zubieta and P.R. Raithby, Cryst. Struct. Commun., 11 (1982) 1945.

17 (a) B.K. Blackburn, S.G. Davies, K.H. Sutton and M. Whittaker, Chem. Soc. Rev., 17 (1988) 147; (b) J.M. Brown and P.L. Evans, Tetrahedron, 44 (1988) 4905; (c) R.A. Gates, M.F. D'Agostino, K.A. Sutin, M.J. McGlinchey, T.S. Janik and M.R. Churchill, Organometallics, 9 (1990) 20; (d) C.E. du Plooy, C.F. Marcus, L. Carton, R. Hunter, J.C.A. Boeyens and N.J. Coville, Inorg. Chem., 28 (1989) 3855.

18 CHEM-X, developed and distributed by Chemical Design Limited, Oxford, England.
19 For a similar approach, P.D. Harvey, W.P. Schaefer, H.B. Gray, D.F.R. Gilson and I.S. Butler, Inorg. Chem., 27 (1988) 57.
20 S.G. Davies, Pure Appl. Chem., 13 (1988) 60.
21 Only two structure determinations of *cis*-substituted complexes have been reported [22a,b], in neither of which is the substituent an alkyl group; there is thus some uncertainty regarding the degree of bending of the Me group out of the diene plane. Modelling of the cycloheptadiene complex requires an evaluation of the flexibility of the $(CH_2)_3$ bridge [5a,8f].
22 (a) J. Morey, D. Gree, P. Mosset, L. Toupet and R. Gree, Tetrahedron Lett., 28 (1987) 2959; (b) G. Maglio, A. Musco, R. Palumbo and A. Sirigiu, Chem. Commun., (1971) 100.
23 (a) S. Zobi-Ruh and W. von Philipsborn, Helv Chim. Acta., 64 (1981) 2378; (b) A.J. Pearson, Aust. J. Chem., 29 (1976) 1679; (c) D.H. Gibson and T.S. Ong, J. Organomet. Chem., 155 (1978) 221.
24 S.D. Worley, T.R. Webb, D.H. Gibson and T.S. Ong, J. Electron Spectrosc. Relat. Phenom., 18 (1980) 189.
25 For a discussion of σ/π character and steric effects of phosphines, see M.N. Golvin, M.M. Rahman, J.F. Belmonte and W.P. Giering, Organometallics, 4 (1985) 1981.
26 D.L. Cronin, J.R. Wilkinson and L.J. Todd, J. Magn. Reson., 17 (1975) 353.
27 A.R. Rossi and R. Hoffmann, Inorg. Chem., 14 (1975) 365.
28 D.B. Beach, R. Bertoncello, G. Granozzi and W.L. Jolly, Organometallics, 4 (1985) 311.
29 T.A. Albright and R. Hoffmann, Chem. Ber., 111 (1978) 1591.
30 Line shape analysis of the ^{31}P spectra of **10** in CD_2Cl_2 was performed using a program based on I.O. Sutherland, Ann. Rep. NMR Spectroscopy, 4 (1971) 80; line shape analysis of the ^{13}C spectra of (isoprene)$Fe(CO)_3$ was performed using EXCHANGE (R.E.D. McClung, University of Alberta). Observed and calculated spectra are available as supplementary material from the authors.
31 M. Brookhart and D.L. Harris, J. Organomet. Chem., 42 (1972) 441.
32 (Sorbaldehyde)$Fe(CO)_3$ exhibits a low temperature spectrum ($-55°C$; CD_2Cl_2) with CO resonances at 214.0 (axial) and 209.5 and 207.1 ppm (basal); ^{13}C spectra of **6–8** (Table 1), thus show two deshielded basal resonances rather than an axial/basal pair.
33 N.A. Clinton and C.P. Lillya, J. Am. Chem. Soc., 92 (1970) 3058.
34 O. Grummitt and E.I. Baker, Organic Synthesis, Coll. Vol. IV, 771.
35 (a) R.E. Schuster, J.E. Scott and J. Casanova, Org. Synth., 46 (1966) 75; (b) I. Ugi, R. Meyr, M. Lipinski, F. Bodonsheim and F. Rosendahl, ibid., 41 (1961) 13; (c) W.P. Weber and G.W. Gokel, Tetrahedron Lett., (1972) 1637.
36 S.V. Ley, C.M.R. Low and A.D. White, J. Organomet. Chem., 302 (1986) C13.
37 (a) S.D. Ittel, F.A. van Catledge and J.P. Jesson, J. Am. Chem. Soc., 101 (1979) 3874; (b) F.A. van Catledge, J.P. Jesson and S.D. Ittel, J. Organomet. Chem., 268 (1979) C25.
38 G.M. Sheldrick, SHELX86, A Computer Program for Crystal Structure Determination, University of Goettingen, 1986.
39 G.M. Sheldrick, SHELX76, A Computer Program for Crystal Structure Determination, University of Cambridge, 1976.
40 D.T. Cromer and J.B. Mann, Acta Crystallogr. A, 24(1968) 321.
41 R.F. Stewart, E.R. Davidson and W.T. Simpson, J. Chem. Phys., 42 (1965) 3175.
42 D.T. Cromer and D.J. Liberman, J. Chem. Phys., 53 (1970) 1891.
43 M. Sacerdoti, V. Bertolasi and G. Gilli, Acta Crystallogr. B, 36 (1980) 1061.
44 E.J.S. Vichi, P.R. Raithby and M. McPartlin, J. Organomet. Chem., 256 (1983) 111.
45 H. Berke, W. Bankhardt, G. Huttner, J. van Seyerl and L. Zsolnai, Chem. Ber., 114 (1981) 2754.